Title
Genomic and Functional Approaches to Understanding Cancer Aneuploidy

Journal
Cancer Cell, 33(4)

ISSN
1535-6108

Authors
Taylor, Alison M
Shih, Juliann
Ha, Gavin
et al.

Publication Date
2018-04-01

DOI
10.1016/j.ccell.2018.03.007

Peer reviewed

HHS Public Access

Author manuscript

Cancer Cell. Author manuscript; available in PMC 2019 April 09.

Published in final edited form as:

Cancer Cell. 2018 April 09; 33(4): 676–689.e3. doi:10.1016/j.ccell.2018.03.007.

Genomic and Functional Approaches to Understanding Cancer Aneuploidy

Alison M. Taylor[1,2,3], **Juliann Shih**[2], **Gavin Ha**[1,2,3], **Galen F. Gao**[2], **Xiaoyang Zhang**[1,2,3], **Ashton C. Berger**[2], **Steven E. Schumacher**[1,2], **Chen Wang**[4,5], **Hai Hu**[6], **Jianfang Liu**[6], **Alexander J. Lazar**[7], **The Cancer Genome Atlas Research Network**, **Andrew D. Cherniack**[1,2,3], **Rameen Beroukhim**[1,2,3], and **Matthew Meyerson**[*,1,2,3]

[1]Department of Medical Oncology, Dana-Farber Cancer Institute, 450 Brookline Avenue, Boston, MA 02215, USA

[2]Cancer Program, Broad Institute, 415 Main Street, Cambridge, MA 02142, USA

[3]Harvard Medical School, 25 Shattuck Street, Boston, MA 02115, USA

[4]Department of Health Sciences Research, Mayo Clinic College of Medicine, 200 First Street SW, Rochester, MN 55905, USA

[5]Department of Obstetrics and Gynecology, Mayo Clinic College of Medicine, 200 First Street SW, Rochester, MN 55905, USA

[6]Chan Soon-Shiong Institute of Molecular Medicine at Windber, Windber, PA 15963

[7]Departments of Pathology, Genomic Medicine, and Translational Molecular Pathology, The University of Texas MD Anderson Cancer Center, 1515 Holcombe Blvd-Unit 85, Houston, Texas, USA

Summary

Aneuploidy, whole chromosome or chromosome arm imbalance, is a near-universal characteristic of human cancers. In 10,522 cancer genomes from The Cancer Genome Atlas (TCGA), aneuploidy was correlated with *TP53* mutation, somatic mutation rate, and expression of proliferation genes. Aneuploidy was anti-correlated with expression of immune signaling genes, due to decreased leukocyte infiltrates in high-aneuploidy samples. Chromosome arm-level alterations show cancer-specific patterns, including loss of chromosome arm 3p in squamous

[*]Corresponding author and lead contact, matthew_meyerson@dfci.harvard.edu.

Declaration of Interests

M.M., A.D.C., A.C.B., and G.F.G. receive research support from Bayer HealthCare Pharmaceuticals. M.M. is a consultant for and equity holder in OrigiMed. R.B. consults for and receives research support from Novartis. Other authors declare no competing interests.

Author Contributions

A.M.T., J.S., G.H., G.F.G., A.C.B., S.S., H.H., and J.L. performed computational analyses; A.M.T. and X.Z. performed *in vitro* experiments and sequencing; TCGA Research Network provided genomic data of patient samples; A.D.C., R.B., and M.M. supervised the work; C.W. and A.J.L. provided feedback and advice on analyses; A.M.T. and M.M. wrote the manuscript.

cancers. We applied genome engineering to delete 3p in lung cells, causing decreased proliferation rescued in part by chromosome 3 duplication. This study defines genomic and phenotypic correlates of cancer aneuploidy and provides an experimental approach to study chromosome arm aneuploidy.

Graphical abstract

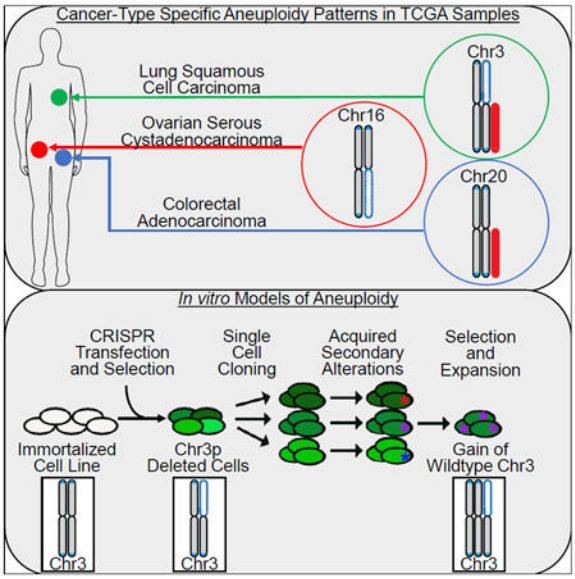

Keywords

aneuploidy; cancer genomics; genome engineering; lung squamous cell carcinoma

Introduction

Aneuploidy, an unbalanced number of chromosomes, was first observed in tumor cells over 100 years ago (reviewed in Holland and Cleveland, 2009) and is a predominant cancer feature occurring in ~90% of solid tumors (Weaver and Cleveland, 2006). Even though it is the among the oldest described cancer alterations, and even though genomics efforts have allowed high-throughput “karyotyping” of patient cancers, the role of aneuploidy in tumorigenesis is still a mystery.

Aneuploidy and focal copy number alterations represent two classes of somatic copy number alteration (SCNA) (Tang and Amon, 2013). Studies of genomic and phenotypic correlates of aneuploidy and SCNAs have examined copy number based on cytoband (Carter et al., 2006) or based on number of SCNAs, including broad and focal events (Davoli et al., 2017; Buccitelli et al, 2017). By these definitions, increased SCNA levels were reported to correlate with proliferation pathways (Carter et al., 2006; Davoli et al., 2017; Buccitelli et al., 2017) and to anti-correlate with immune signaling within individual tumor types (Davoli et al., 2017; Buccitelli et al., 2017).

We define aneuploidy as SCNAs of whole chromosomes and of chromosome arms. In cancer, aneuploidy affects more of the genome than any other somatic genetic alteration (Beroukhim et al., 2010; Zack et al, 2013; Mitelman, 2000). The most frequent recurrent arm alterations occur in over 30% of tumors, whereas the most frequent recurrent focal copy number alterations occur at a frequency below 0.15 (Beroukhim et al., 2010). Chromosome arm SCNAs are more common than whole chromosome SCNAs, occurring at higher frequencies in 12 of 16 cancer types analyzed (Beroukhim et al., 2010). Cancer subtypes are often characterized by tumor-specific patterns of chromosomal arm-level alterations (Ried et al., 2012), including squamous subtypes of lung, esophageal, and bladder tumors (Hoadley et al., 2014). Specific chromosome arm level alterations have also defined groups of tumors that are responsive to particular therapies, such as low grade gliomas with 1p/19q co-deletions that have been shown to be responsive to specific chemoradiotherapy regimens (Cairncross et al., 2013).

The functional effect of an individual aneuploidy is often thought to be due to the deletion of a tumor suppressor or overexpression of an oncogene (Liu et al., 2016). However, increasing evidence suggests that the effects of broad SCNAs result from the alteration of a combination of genes (Xue et al., 2012; Bonney et al., 2015). Recent SCNA models suggest that the phenotypic effect of chr_17p loss is due to more than *TP53* loss of heterozygosity (Liu et al., 2016). Chr_3p loss is an early event in lung squamous cell carcinoma observed in preneoplastic regions in the lung (Hung et al., 1995; Sundaresan et al., 1992), yet studies suggest that its contributions to tumor development are not the result of loss of one gene (Wistuba et al., 2000).

To study the role of aneuploidy in tumor development, models of whole chromosome aneuploidy have been developed. Trisomies and monosomies have been extensively modeled in yeast, where they slow proliferation and induce proteosomal stress (Torres et al., 2007; Sheltzer et al., 2011). Mouse cells with Robertsonian translocations can be used to model one trisomy at a time (Williams et al., 2008), or cells can be compared that differ only by single chromosomes added by microcell-mediated cellular transfer (Sheltzer et al., 2017; Stingele et al., 2012). These studies also show that whole chromosome aneuploidy leads to cellular senescence and decreased proliferation and transformation capabilities; however, karyotype evolution can lead to a rescue of proliferation rates (Sheltzer et al., 2017). There is one characterized model of targeted chromosome arm-level deletion, where chromosome arm 8p was deleted in mammary epithelial cells by targeting TALENs at either end of the chromosome arm and screening for recombination (Cai et al., 2016). In this model, 8p deletion does not lead to an increase in growth rate or tumorigenic potential.

Recent advances in targeting of endonucleases allow approaches to generating broad chromosomal alterations *in vitro*. Cas9-CRISPR (clustered regularly interspaced short palindromic repeats) systems are particularly advantageous for their high efficiency and design tools available for targeting DNA throughout the genome (Mali et al., 2013; Hsu et al., 2013). CRISPR-targeting, when combined with an artificial telomere-containing plasmid, can be used to truncate a chromosome arm (Uno et al., 2017).

Here, we apply methods that define chromosome arm-level aneuploidy and a global cancer aneuploidy score to 10,522 tumors of 33 types in the Cancer Genome Atlas (TCGA), and develop and analyze an experimental cellular model for chromosome arm-level aneuploidy. By combining analysis of highly annotated cancer genomes and the experimental ability to manipulate chromosomes, we can advance our understanding of the effects of aneuploidy and specific chromosome arm-level alterations in cancer development and progression.

Results

Generation of aneuploidy scores for 10,522 TCGA cancers

To study features associated with aneuploidy, we first generated an aneuploidy score reflecting the total number of chromosome arms with arm-level copy-number alterations in a sample. When identifying these arm-level alterations, we were cognizant that two SCNAs that did not overlap could be misconstrued as a single event if we simply tallied arms with more than 50% of their length altered – for instance, if the SCNAs originated on opposite ends of the chromosome arm. Conversely, a simple length cutoff might exclude smaller SCNAs even if they cover most of the genomic region covered by larger SCNAs called as arm-level events (Figure S1A). We therefore clustered SCNAs on each arm based upon their locations and lengths (using a Gaussian mixture model) to identify events with likely similar consequences (Figure S1B and Method S1). Clusters in which the mean length of that SCNA was greater than 80% of the chromosome arm were considered positive for an arm alteration, samples whose SCNA length was less than 20% of a chromosome arm were considered negative, and clusters whose SCNAs were of intermediate length were not called.

We applied this approach to 10,522 samples spanning 33 cancer types from The Cancer Genome Atlas (TCGA) pan-cancer dataset (Table S1). Somatic DNA copy number was determined from Affymetrix SNP 6.0 arrays profiling of tumor samples. From SNP array data and mutational data, we used the ABSOLUTE algorithm (Carter et al., 2012) to generate segmented absolute copy number and estimate sample purity, ploidy, and number of whole genome doublings. SCNAs, identified by ABSOLUTE to be clonal, were called as deviations from the euploid level of the sample: we considered a purely tetraploid cell (identified in 18 samples in our analysis) as having no arm-level SCNAs. (See STAR Methods and Table S1 for additional information about expression and mutation data.) Using this arm-calling approach, we determined the arm-level SCNA status of more than 400,000 chromosome arms and more than 175,000 non-acrocentric whole chromosomes for the 10,522 cancer genomes (Table S2).

Next, we calculated an aneuploidy score that reflects the total burden, or number, of arm-level events in each sample. This aneuploidy score ranged from 0 to 39, the total number of human autosomal chromosome arms: p and q arms for chromosomes 1-12 and 16-20, together with q arms for the acrocentric chromosomes 13-15 and 21-22 (Figure 1A, Figure S1C). Previous studies have demonstrated that there is less than a two-fold change in frequency of arm alteration due to arm length (Beroukhim et al., 2010), and our aneuploidy score highly correlates with fraction of genome altered by aneuploidy (Spearman’s rank correlation coefficient = 0.975, Figure S1D). For these reasons, we chose the sum of arms altered for subsequent analyses.

Samples that have undergone whole genome doubling, as defined by ABSOLUTE, have a higher degree of aneuploidy (Spearman's rank correlation coefficient = 0.55), suggesting that tumors with increased ploidy are more prone to aneuploidy events (Figure 1B). However, among samples of the same genome doubling status, increased aneuploidy is generally associated with decreasing ploidy, indicating that the arm-level events that contribute to aneuploidy are more often absolute losses than gains (Figure 1C).

Across the entire sample panel, 88% of cancers had at least some detectable aneuploidy (mean aneuploidy score of 10.0); however, this rate varied substantially across cancer types (s.d. between cancer type aneuploidy means = 4.8; Figure 1D). For example, only 26% of thyroid carcinomas have any chromosome arm-level alteration (mean aneuploidy score of 0.87), and less than half of acute myeloid leukemias and thymomas have these alterations (mean aneuploidy scores of 1.6 and 3.8, respectively). In contrast, virtually all glioblastomas (99%, mean aneuploidy score of 8.2), uterine carcinosarcomas (96%, mean aneuploidy score of 17.2), and testicular germ cell tumors (99%, mean aneuploidy score of 18.7) have at least one aneuploidy event (Figure 1D).

Relationship between cancer mutation frequencies and aneuploidy

A variety of studies have assessed the relationship between chromosomal copy number alteration and somatic mutation (Ciriello et al., 2013; Zack et al., 2013; Davoli et al., 2017). We applied the aneuploidy scores of the full pan-cancer cohort of TCGA cases to examine this relationship. To assess whether gene mutations are associated with aneuploidy, we used a multivariable linear regression model that accounts for cancer type and the number of mutations per sample.

In this analysis, *TP53* was an outlier, with the highest coefficient in the linear model (towards enrichment of mutations among aneuploid samples) and the highest statistical significance (Figure 2A, Table S3), consistent with previous studies (Ciriello et al., 2013; Zack et al., 2013; Davoli et al., 2017). We also detected significant associations between aneuploidy and mutation rate for 34 other genes. However, the correlation coefficients for these genes were always negative (towards enrichment of mutations in low aneuploidy samples) and never exceeded a magnitude of 0.027, whereas the coefficient for *TP53* was positive 0.13.

Next, we assessed the relationship between somatic mutation rate and aneuploidy. It has been previously reported that there is an inverse relationship between the frequencies of recurrent copy number alterations and of recurrent somatic mutations in cancer (Ciriello et al., 2013; Figure S2A). While we do also observe that cancers with very high mutation rates have low aneuploidy scores (Figure 2B), these high mutation rate/low aneuploidy cancers largely exhibit high levels of microsatellite instability or *POLE* mutation, primarily in colon adenocarcinoma and endometrial cancers (Figure 2B).

In contrast, when these hypermutated tumors are excluded, we observed a positive correlation between mutation frequency and aneuploidy score (Spearman's rank correlation coefficient = 0.38), as well as between recurrent SCNAs and recurrent mutations (Spearman's rank correlation coefficient = 0.34). The positive correlation between mutation

and aneuploidy was found in most cancer types with the notable exceptions of colorectal carcinoma (COAD and READ) and uterine carcinoma (UCEC and UCS) as well as uveal melanoma (UVM) and stomach adenocarcinoma (STAD) (Figure 2C, Table S4). All of these exceptions other than uveal melanoma had some cases of microsatellite instability or *POLE* mutation.

Relationship between immune infiltrates and aneuploidy

Another important question about the cancer genome is the relationship between genome alterations and the immune response. Tumor mutational burden is known to be associated with response to immune checkpoint inhibition in cancer (Topalian et al., 2016; Rizvi et al., 2015), while aneuploidy has been reported to be associated with decreased immune infiltrate across many tumor types (Davoli et al., 2017). To assess the relationship between aneuploidy and immune infiltrates, we performed analyses of gene expression as a function of aneuploidy scores. The contribution of cells such as fibroblasts, leukocytes, endothelial cells, and other cell types is a confounding factor in the analysis of gene expression in primary tumors, so we also controlled for these features in our analysis. We measured immune and stromal cell populations using computational analyses rather than pathology-based estimates, as sections of the tumor used for histology were different from those used for molecular profiling. For estimating purity, we used ABSOLUTE, an established copy number pipeline used in most TCGA studies that has been benchmarked histologically (Carter et al., 2012; Zack et al., 2013). For leukocyte fraction, estimates based on methylation (TCGA PanCanAtlas immune paper, submitted) and expression (Aran et al., 2017) correlate with a Spearman's rank correlation coefficient of 0.706 (Figure S2B). Namely, we first identified features reflecting cellular composition that associated with aneuploidy, and included these in our regression model tying gene expression to aneuploidy.

We first found that cancer impurity, as measured by ABSOLUTE (Carter et al., 2012), positively correlated with aneuploidy; in other words, cancers with high aneuploidy were associated with a higher fraction of non-cancerous cells (Figure 3A, Table S4). However, the measurement of leukocyte fractions based on methylation signatures, as previously described (Carter et al., 2012; TCGA Immune Subgroup, submitted), showed a negative correlation with aneuploidy (Figure 3B, Table S4). Most individual tumor types showed a negative correlation between aneuploidy and leukocyte fraction, which was strongest in pancreatic adenocarcinoma and head and neck squamous cell carcinoma (Spearman's rank correlation coefficients = -0.428 and -0.312, respectively) (Figure 3B, Table S4). This observation is consistent with previous reports that aneuploidy is associated with decreased levels of cancer immune infiltrate (Davoli et al., 2017). Paradoxically, pan-cancer analysis shows a slight positive correlation between aneuploidy score and leukocyte fraction (Spearman's rank correlation = 0.0568, Figure S2C), but this is driven by differences between tumor types as there is a negative correlation within most tumor types (Figure S2D). Combining the aneuploidy and leukocyte fraction results, the observed positive correlation of aneuploidy with impurity could be related to a non-leukocyte cellular fraction that is associated with aneuploidy (Figure 3C, Table S4).

Another way to assess immune infiltrates is by gene expression rather than methylation data. Using RNA sequencing data from 9,670 TCGA cancers for which there was also aneuploidy data (Table S1, STAR Methods), we generated a linear regression model relating the expression of each gene (measured by RSEM values of RNA sequencing data) in each sample as a function of aneuploidy score, across all cancer types (Table S5). A ranked list of significant aneuploidy score coefficients for each gene was analyzed by gene set enrichment (GSEA) with the MSigDB hallmark gene sets.

In the case of univariate linear regression, we observed a statistically significant (FWER p value < 0.01) enrichment for proliferation pathways (such as E2F targets, mitotic spindle, and G2M checkpoint) and immune pathways (including interferon gamma response, allograft rejection, and immune response) (Figure 3D, column 1, Table S6). At first glance, this result appears contradictory to previously published studies (Davoli et al., 2017; Buccitelli et al., 2017). However, when we added tumor type as an additional variable in the linear regression model, immune gene sets were negatively associated with aneuploidy scores (Figure 3D, column 2, Table S6), consistent with other studies that assessed correlations within specific tumor types (Davoli et al., 2017, Buccitelli et al., 2017). When calculating an immune gene set expression score per sample, we also observed a pan-cancer positive correlation which is driven by tumor type, consistent with the linear regression model (Figure S2E, S2F).

To determine if the purity and immune infiltrate factors contribute to the aneuploidy correlated expression patterns, we added them to our linear model. Adding purity or non-leukocyte stroma as variables did not affect the enrichment of immune signatures (Figure 3D, columns 3 and 4, Table S6), but addition of leukocyte fraction as a variable resulted in the loss of the immune signature enrichment (Figure 3D, column 5, Table S6). These results suggest that the enrichment of the immune expression signature was due to the fraction of leukocyte infiltrate present in that sample. In contrast, pro-proliferative and cell cycle pathways were significantly positively correlated with aneuploidy score, regardless of other predictors in the model (Figure 3D, Table S6).

Cancer-type-specific patterns of chromosome arm-level aneuploidies

Next, we assessed the rates of whole chromosome and chromosome arm alteration across human cancer types. Arm or whole chromosome alterations occurred in 88% of cancer samples. Not including acrocentric chromosomes, whole chromosome alterations occurred in 66% of samples and chromosome arm-level alterations occurred in 78% of samples (Table S2). Individual arms and chromosomes were altered at different frequencies (Table S7); 8p and 17p were the most frequently deleted (at 33% and 35%, respectively), 8q was the most commonly gained (33% of samples), and 2p and 2q the least commonly altered (total 18% and 16%, respectively). Chromosome arms 6p, 12q, 17q, and 19q were gained and lost in equal percentages (difference between gain and loss frequency < 0.03), but others were predominantly gained (1q, 7p, 8q, and 20q) or predominantly lost (3p and 17p).

We observed that every cancer type harbors a unique pattern of aneuploidy, with different arms or whole chromosomes altered at different frequencies (Table S7). To compare different cancer types and molecular subtypes, we performed hierarchical clustering of mean

arm-level calls (Figure 4A, Table S8), previously performed across 3,000 TCGA samples (Beroukhim et al., 2010). Within an individual cancer type, molecular subtypes often clustered together, such as glioblastoma subtypes and testicular germ cell tumor subtypes (Figure S3A). Consistent with previous analyses, endometrial cancer was a notable exception, as copy number high “serous like tumors” cluster separately from other endometrial subtypes (Figure 4A and TCGA, 2013). Testicular germ cell tumors were characterized by chromosome 12p gain among other aneuploidy events (Taylor-Weiner et al., 2016). Glioblastomas without IDH mutations are characterized by chromosome 7 gain and chromosome 10 loss, consistent with previous studies (Brennan et al., 2013). Low grade gliomas cluster near glioblastomas, but are characterized by distinct alterations of chromosome 1p loss and chromosome 19q gain correlating with IDH mutation (TCGA, 2015), a pattern shown to be therapeutically relevant (Cairncross et al., 2013).

Several cross-tumor clusters emerged from our analysis (Figure 4A, Table S8). Gastrointestinal tumors (colorectal, non-squamous esophageal, stomach, and pancreatic) clustered together with co-occurring gains of 8q, 13q, and chromosome 20, regardless of the status of microsatellite or chromosome instability. We also observed a cluster of some gynecological tumors (ovarian cancer and endometrial cancers with high copy number alterations) and a second cluster of epithelial tumors characterized by 1q gain (lung adenocarcinoma, breast cancers, and liver hepatocellular carcinoma). Neural lineage cancers (low grade glioma, glioblastoma, and melanoma) formed a cluster neighboring additional mesoderm-derived tumors (endometrial cancers with few copy number alterations, renal clear cell carcinoma, and renal papillary cell carcinoma), characterized by recurrent chromosome 7 gain and fewer aneuploidy alterations.

Previous clustering efforts by multiple data types across 12 tumor types showed that squamous cancers from different tissues of origin (lung, esophagus, and bladder) clustered together (Hoadley et al., 2014). Our analyses also separated out squamous cancers based on aneuploidy data alone, suggesting that broad SCNAs are a major determinant of the squamous cluster. A dominant feature of the squamous cancer cluster was chromosome arm 3p loss and chromosome arm 3q gain, which is present in cervical squamous cell carcinomas (CESC) and HPV positive head and neck squamous cell carcinomas (HNSC), and strongest in esophageal squamous cell carcinomas (ESCC), lung squamous cell carcinoma (LUSC) and HPV negative HNSC squamous tumors.

Chromosome 3 alterations are a known feature of lung squamous cell carcinoma (Bass et al., 2009; Hagerstrand et al., 2013; Zabarovsky et al., 2002), with chromosome 3p loss present in preneoplastic lesions in the lung (Hung et al., 1995; Sundaresan et al., 1992). In our lung squamous cell carcinoma dataset, chromosome 3p was deleted in almost 80% of tumors and chromosome arm 3q was gained in over 60% of tumors (Figure 4B). The co-occurrence of chr_3p loss and chr_3q gain was significantly more frequent than would be expected by chance (Figure 4B; chi-square $p = 0.0386$). Alterations in the reverse direction, chr_3p gain and chr_3q loss, were not observed in our dataset. In contrast, in lung adenocarcinoma, less than half of tumors had 3p loss and only 13% had 3q gain (Campbell et al., 2016), and these did not significantly co-occur ($p=0.0626$). Chr_3p gains occurred, though rarely, and chr_3q loss occurs at higher rates. As expected, deletion of 3p correlated with a reduction of 3p

gene expression across TCGA samples (Figure S3B). Based on the linear modeling of gene expression, chr_3p alteration negatively correlated with hallmark sets of cell cycle (E2F targets/G2M Checkpoint, Figure S3C, FWER p value < 0.01), epithelial mesenchymal transition, interferon gamma response, and TNFa signaling (Figures S3D and S3E, FWER p value < 0.01). These pathways were down-regulated when 3p is gained and up-regulated when 3p is lost.

Genome engineering approach to delete chromosome arm 3p *in vitro*

Chromosome arm-level aneuploidies occur in almost 80% of cancers, yet have been rarely modeled in human cells (Cai et al., 2016; Uno et al., 2017). Given the continuing scientific mystery regarding the function of cancer aneuploidy, and given that deletion of chromosome 3p occurs in almost 80% of squamous cell lung cancers, we wanted to further understand the effect of chr_3p deletion in lung epithelial cells. We developed a recombination directed approach to remove the 3p chromosome arm. Using the CRISPR-Cas9 system, we generated double strand breaks (DSBs) centromeric to all genes on the 3p arm. We modified a plasmid containing an artificial telomere and puromycin selection cassette (Uno et al., 2017) by addition of one kilobase DNA of sequence homologous to the region centromeric of the chr_3p DSB (Figure 5A). The CRISPR plasmid and telomere-containing plasmid were co-transfected into cells, and the recombination event was selected for with puromycin treatment. We observed successful recombination verified by Sanger sequencing, in a human immortalized lung epithelial cell line (AALE, immortalized by SV40 large T antigen) (Figure S4A). To test for chr_3p hemizygous deletion, we performed quantitative PCR (qPCR) on genomic DNA to compare chr_3p and chr_3q levels. Single cell clones that were positive for recombination were positive for chr_3p hemizygous deletion by qPCR (Figure 5B), as well as whole genome sequencing (Figure 5C and Figure S4B) and karyotyping (Figure 5D).

Chromosome arm 3p deleted cells evolve over time

We evaluated the growth of cells with chromosome 3p truncation (Figure 6A). At the first round of characterization, ten passages post-single cell cloning, chromosome 3p deleted cells proliferated more slowly than their non-deleted siblings (Figure 6B, p value < 0.05). The chr_3p hemizygously deleted cells did not undergo increased apoptosis as measured by propidium iodide staining (Figure S4C). However, we observed more cells in G1 of the cell cycle by propidium iodide staining in fixed cells, indicative of cell cycle arrest (Figure S4D, p value < 0.001). AALE parental cells do not form colonies in soft agar (Lundberg et al., 2002), and 3p deleted cells were also negative in this assay for anchorage independent growth (data not shown). RNA sequencing of deleted clones and their non-deleted siblings confirmed down-regulation of chr_3p genes in *cis*, statistically significant for 64% of genes (FDR < 0.05) (Figure S4E). *STAC* and *ROBO1* were the most down-regulated 3p genes, decreased by more than 15-fold, and chr_3p genes *UBA7* and *LMCD1* were up-regulated more than two-fold. Chr_3p hemizygously deleted cells also had up-regulation of interferon and immune response pathways by GSEA (FWER < 0.01) (Figure 6C), consistent with the finding that 3p copy number was anti-correlated with these pathways in the pan-cancer analysis (Figures S3D and S3E).

After an additional 4-5 passages (approximately 10 population doublings) and one round of freeze-thaw, 3p deleted cells no longer proliferated more slowly (Figure 6D). 53% of chr_3p genes were still significantly down-regulated (FDR < 0.05) (Figure S4F), with *STAC* and *ROBO1* decreased more than 13-fold. Interestingly, *UBA7*, an ubiquitin enzyme on 3p which targets interferon gene *ISG15*, was no longer up-regulated. By GSEA, interferon pathways were still up-regulated (Figure 6C), though enrichment scores were lower and other immune signatures were no longer significant. Later stage chr_3p deleted cells had downregulation of genes involved in the epithelial mesenchymal transition and angiogenesis (GSEA FWER < 0.01), but the implications of this remain obscure. We also observed subclones with duplication of the remaining full copy of chromosome 3 in two of the three deleted clones (Figure 6E, Figure S4G). In these subclones with chromosome 3 duplications, 3q is gained and 3p is no longer lost. We conclude that selection of advantageous alterations or expression changes allow chr_3p deleted cells to overcome the negative growth effects of aneuploidy in this model system (Figure 6F). In this section, we have demonstrated that it is possible to model aneuploidy. We have not observed a neutral or positive impact of aneuploidy on cell proliferation. Results are summarized in Table 1.

Discussion

Here, we present parallel computational and experimental approaches that provide insight into the largely unexplored role of aneuploidy in cancer. By calculating aneuploidy level in 10,522 tumors, we uncovered the correlation of aneuploidy with *TP53* mutations, overall somatic mutation rate, and proliferative signatures, and an inverse correlation with leukocyte fraction. Our analysis revealed expression changes in cell-cycle and immune hallmarks associated with individual chromosome arm-level alterations, independent of aneuploidy level. We also observe tissue specific patterns of aneuploidy, and squamous tumors of different tissue origins clustering together. Using CRISPR technology, we modeled one of the chromosome arm alterations observed in squamous tumors (chr_3p deletion) in human immortalized lung epithelial cells. A decrease in cellular proliferation rate is associated with chr_3p deletion, a phenotype that is reversed by gain of chromosome 3.

Examining pan-cancer aneuploidy analyses

In this study, we defined aneuploidy to include chromosome and arm-level somatic copy number alterations (SCNAs), but not smaller SCNAs. In some cases, computationally derived definitions of aneuploidy and analyses of SCNAs have included both broad and focal SCNAs (Davoli et al., 2017; Buccitelli et al., 2017). Broad and focal events occur by different mechanisms and have different effects; broad events affect a large number of genes by one or few copies, while focal events affect fewer genes with higher amplitudes of gain or with homozygous deletion (Beroukhim et al., 2007). Therefore we chose to restrict our analysis to the broad events, to harmonize the definition of aneuploidy more with the mechanism of generation of the structural and transcriptional consequences.

Aneuploidy level varies greatly across tumor type, impacting the analyses of aneuploidy correlations with mutation rate and immune signatures and potentially leading to conflicting results in the literature (Ciriello et al., 2013; Davoli et al., 2017; Buccitelli et al., 2017). By

controlling for tumor type, as well as confounders such as sample purity and cellular composition, our analysis reconciles discrepancies in the literature. Regarding mutation rate and aneuploidy correlations across cancers, mutation rate is inversely proportional to aneuploidy, but this anti-correlation is driven by tumors with high microsatellite instability (MSI, mostly colon adenocarcinoma and endometrial cancers). Once MSI tumors are removed, mutation and aneuploidy are positively correlated (consistent with Davoli et al., 2017 and Buccitelli et al., 2017).

When controlling for tumor type, our results are consistent with a negative correlation between aneuploidy and leukocyte infiltrate that explains a decrease in expression of immune signatures. Interestingly, some studies have shown that abnormal karyotypes or hyperploidy can trigger an immune response (Santaguida et al., 2017; Senovilla et al., 2012). This result suggests the possibility that aneuploid tumor cells may have to overcome or evade this ploidy-related immune response for tumors to progress.

When controlling for tumor type, aneuploidy level, and cellular composition of each sample, we identified immune expression signatures that can independently correlate with individual arm-level copy number alterations. Deletions of some arms, including 3p, 8p, 13q, or 17p, are positively correlated with immune signatures, whereas deletions of other arms, including 4q, 5q, and 14q, are anti-correlated with immune signatures. The distinct correlations of immune signatures with deletion of different arms also suggest that immune signature changes might be due to specific genes or regions within each affected arm rather than to overall aneuploidy.

Genome engineering to model an individual cancer aneuploidy

We have developed a method to generate chromosome arm deletions by initiating centromeric DNA breaks with CRISPR/Cas9 to promote replacement of an arm with a selection cassette and an artificial telomere. The method described here can be applied to deletion of any chromosome arm. In the case of chr_3p deletion, differential expression of chr_3p genes and interferon response genes is consistent with expression changes across TCGA samples, supporting the utility of both our computational and experimental approaches.

Consistent with single chromosome aneuploidy models in human cells (Stingele et al., 2012; Sheltzer et al., 2017), chromosome arm-level deletion of human chr_3p has an anti-proliferative effect that cells can overcome with time. Even though p53 is inhibited in the lung epithelial cells, as they were immortalized with SV40 large T antigen (Lundberg et al., 2002), chr_3p deletion initially caused a decrease in cell proliferation. We initially predicted that deletion of chr_3p would not be as anti-proliferative as other aneuploidies, as it is thought to be an early event in lung tumorigenesis (Hung et al., 1995; Wistuba et al., 2000). However, in our cells, selective pressures have likely induced some secondary changes in the chr_3p deleted cells to promote proliferation.

One previously observed mechanism of selection is the evolution of cell line karyotypes over time (Sheltzer et al., 2017). In two of the three chr_3p deleted clones, we observed subclones with a duplicated wildtype copy of chromosome 3, changing an individual cell

from chr_3p deleted to chr_3q gained. Interestingly, chr_3q gain is also a defining feature of squamous cell carcinoma, and contains oncogenes such as *SOX2, PIK3CA*, and *TERC*. In the future, we plan to expand our chromosome deletion model to different chromosome arms (Cai et al., 2016; Uno et al., 2017), and thereby to interrogate how specific aneuploidies can induce distinct expression patterns, phenotypes, and selection mechanisms.

Open questions in aneuploidy: Tissue specificity and selection

The tissue specificity we observe in patterns of aneuploidy could be due to the specific transcriptional effects of different aneuploidies. Our work here begins to analyze expression changes induced by each arm alteration while controlling for overall aneuploidy level and other confounders. By focusing our analysis within tumor types and comparing between them, we can uncover whether specific aneuploidies have different transcriptional consequences in different tissues. Determining whether transcriptional consequences have distinct selective advantages and disadvantages in different tissues will require further integration of *in vitro* models and computational analysis. In addition, specific aneuploidies may trigger unique dependencies; future directions involve interrogating existing *in vitro* CRISPR and shRNA cell line data to identify potential therapeutic targets that can be validated in the *in vitro* models.

The major question about cancer aneuploidy remains open: is aneuploidy positively selected for in cancer? We favor the view that aneuploidy is positively selected for, as it is a universal and tissue-consistent feature of epithelial cancer. However, the experimental data on cancer aneuploidy do not currently support this model. There are a few possible explanations for this contradiction. In the case of oncogenic mutations, overexpression in model systems often leads to oncogene-induced senescence (Larsson, 2011); individual aneuploidies may elicit a similar response. In addition, we have not yet identified the exact environment for positive selection of aneuploidy; p53/RB inhibition and *TERT* activation may not be sufficient to allow selection of aneuploidies. Future work will involve combining models of diverse aneuploidy events, including chromosome arm gains and losses, along with different mutations and different cellular contexts. It will be increasingly important to incorporate models of stromal interaction into prospective studies of aneuploidy and its selection, whether by advanced cellular modeling, single cell sequencing, or use of animal models. In particular, CRISPR manipulation in human lung organoids will be a useful approach to assess interactions of different lung cell types with aneuploidy alterations, as well as potential stromal cell interactions in a 3D tissue model (Barkauskas et al., 2017). Continued integration of computational and experimental approaches will be required to understand how an aneuploidy alteration, affecting hundreds of genes simultaneously, results in an aneuploidy phenotype and contributes to tumor development or, alternatively, is an unselected event.

STAR Methods

Contact for Reagent and Resource Sharing

Further information and requests for resources and reagents should be directed to and will be fulfilled by the Lead Contact, Matthew Meyerson (matthew_meyerson@dfci.harvard.edu).

Experimental Model and Subject Details

All *in vitro* experiments were performed in XX immortalized lung epithelial cells (AALE cells), derived at Dana-Farber and immortalized by SV40 large-T antigen (Lundberg et al., 2002). Cells were maintained at 37 degrees Celsius and 5% CO_2 in Lonza small airway growth medium (CC-3118).

Method Details

Pan-cancer Computational Analyses

Datasets: For 10,522 TCGA samples, somatic DNA copy number was determined from Affymetrix SNP 6.0 arrays. For 9,670 of these 10,522 samples, RSEM (relative standard error of the mean) expression values were determined from Illumina mRNA sequencing data. For 9,756 of these 10,522 samples, mutations were called from whole-exome DNA sequencing data (TCGA MC3 manuscript, in preparation). (See also Table S1.)

Calculating Arm-Level Events and Aneuploidy Score: Using the ABSOLUTE algorithm (Carter et al., 2012) for each sample, we determined the likeliest ploidy and absolute total copy number of each segment in the genome. Each segment was designated as amplified, deleted, or neutral based on whether its copy number was greater than, smaller than, or equal to the sample's ploidy (rounded to the nearest integer) respectively. For amplifications and deletions separately (collectively "alterations"), segments were joined until either the entire chromosome was considered altered or more than 20% of the genomic length between the start and ends were not altered in the same direction; e.g. >20% deleted or neutral for joining amplification segments. For every combination of arm/chromosome and direction of alteration within each TCGA tumor type, the start coordinates, end coordinates, and percentage length of the longest joined segment were clustered across samples using a Gaussian Mixture Model (Pedregosa et al., 2011, Python package SciKit-Learn). The optimal clustering solution between 2-9 clusters inclusive was chosen based on the lowest BIC (Bayesian information criterion). Tumors in clusters whose mean fraction altered in either specific direction was >=80% were considered "aneuploid." Tumors altered <20% (in both directions) were considered "non-aneuploid," and others were designated "other." Each arm was assigned -1 if lost, +1 if gained, 0 if non-aneuploid, and "NA" if other. Aneuploidy score (number of altered arms) for each tumor is calculated as the sum total of altered arms, for a range of 0 (no arms) to 39 (all arms – long and short arms for each non-acrocentric chromosome, and only long arms for chromosomes 13, 14, 15, 21, and 22).

Other scores: Fraction of genome altered by aneuploidy was determined by multiplying each arm altered by its length, and dividing by the length of the genome. Recurrent SCNA scores are the sum of recurrent SCNAs as identified by GISTIC2.0 (output to be available at NCI Genomic Data Commons). Recurrent mutation scores are the sum of recurrent mutations, defined in the TCGA MC3 manuscript (TCGA, in preparation).

Spearman Correlations: Spearman correlation coefficients were calculated using the spearmanr function in the stats package of scipy-0.19.0, which was run using Python-3.5.4 or using cor.test in R (method = "spearman"), which was run using R version 3.2.3.

Linear Modeling: Linear modeling was performed in R version 3.2.3, using lm. The equations used:

$$\text{Expression}_{(\text{gene X})} \sim \beta_1 * \text{predictor variable} + \beta_2 * \text{aneuploidy score}$$

$$\text{Mutation}_{(\text{gene X})} \sim \beta_1 * \text{predictor variable} + \beta_2 * \text{aneuploidy score}$$

$$\text{Expression}_{(\text{gene X})} \sim \beta_1 * \text{chromosome arm} + \beta_2 * \text{aneuploidy score}$$

P values for each coefficient were calculated by the lm function in R.

Gene Set Enrichment Analysis: Gene set enrichment analysis (GSEA) was performed using Broad GSEA v.3.0 (Subramanian et al., 2005). Ranked lists of genes and coefficients were entered, and enrichment was assessed using Hallmark and Positional Gene Sets.

Clustering: Hierarchical clustering of tissue-means of arm-level alterations was performed using 1-Pearson's in Morpheus (https://software.broadinstitute.org/morpheus/index.html).

Cell Line Analyses

Karyotype Analysis: Karyotype analysis was performed by the Brigham and Women's Cytogenomics Core.

RNA Sequencing and Analysis: RNA was isolated from cells using the Qiagen RNAeasy kit (Qiagen 74104), with DNAse treatment. PolyA isolation and sequencing library preparation was performed using the NEBNext Ultra Directional RNA Library Prep Kit. Each set of samples were pooled and sequenced in one lane of HiSeq2500 RR, 100 basepair paired end. Sequencing reads were aligned using STAR (Dobin et al., 2013) and expression level was quantified by RSEM (Li and Dewey, 2011). Differential expression analysis was performed using the edgeR pipeline (Robinson et al., 2010). Ranked lists of genes with fold change were entered into GSEA as described above.

DNA Sequencing and Analysis: DNA was isolated from cells using the QiaAmp Mini DNA kit. Sequencing library preparation was performed using the Nextera DNA Sample Preparation Kit. Samples were pooled and sequencing by miSeq, 300 basepair paired end. Copy number profiles were generated by HMMCopy (Lai et al., 2016). Subclonal analysis was performed using IchorCNA (Adalsteinsson et al., 2017).

Cell Maintenance, Transfection and Proliferation Assays: Transfections were performed using Fugene-6 (Promega E2691) following manufacturer's instructions at a 3:1 ratio. 24 hours after transfection, cells were selected with 2 μg/mL puromycin through several passages and a round of single cell cloning. For single cell cloning, individual cells were plated in each well of a 96-well plate using cell sorting, with each well containing 100μL of 50% conditioned small airway growth media (SAGM). After single cell cloning and confirmation of telomere recombination, puromycin was no longer added in the media. For cell proliferation assays, 1500 cells per well in a 96-well plate were plated in 100μL of media. Plates were collected at time of plating and days 2, 4, and 6. 50μL of CellTiter-Glo Reagent was added, and plates were incubated for 20 minutes before luminescence readings.

Flow Cytometry: For apoptosis analysis, adherent cells were washed, trypsinized, collected, and stained in propidium iodide solution. Propidium iodide levels were measured on the BD LSRii. For cell cycle analysis, adherent cells were washed, trypsinized, collected, and fixed in 10% formalin buffered solution and 70% ethanol. After fixing, cells were stained with propidium iodide solution for thirty minutes before analysis on the BD LSRii. Cells were assigned to G1, S, and G2 stages of the cell cycle by identifying the G1 peak and 2x G2 peak.

PCR and qPCR: PCR was performed using the Sigma Aldrich AccuTaq enzyme (D8045) with primers listed under key resources. Quantitative PCR (qPCR) was performed using the Power SYBR Green PCR mastermix (ThermoFisher 4367659), with the primers listed above.

Quantification and Statistical Analysis

Quantitative and statistical methods are noted above.

Data and Software Availability

The raw TCGA data, processed data and clinical data can be found at the legacy archive of the GDC (https://portal.gdc.cancer.gov/legacy-archive/search/f) and the PancanAtlas publication page (https://gdc.cancer.gov/about-data/publications/pancanatlas). The mutation data can be found here (https://gdc.cancer.gov/about-data/publications/mc3-2017). TCGA data can also be explored through the Broad Institute FireBrowse portal (http://gdac.broadinstitute.org) and the Memorial Sloan Kettering Cancer Center cBioPortal (http://www.cbioportal.org). For the *in vitro* assays, RNA-sequencing BAM files are available at the Sequence Read Archive as Study PRJNA436953 (SRP133935), Run Numbers SRR6806553-SRR6806554 and SRR6806559-SRR6806570. Related DNA-sequencing BAM files are available at the Sequence Read Archive as Study PRJNA436953 (SRP133935), Run Numbers SRR6806543-SRR6806552 and SRR6806555-SRR6806558. Details for software availability are in the Key Resource Table.

Supplementary Material

Refer to Web version on PubMed Central for supplementary material.

Acknowledgments

All cytogenomics analysis was performed by the CytoGenomics Core at Brigham and Women's Hospital. A plasmid containing an artificial telomere was kindly shared by Narumi Uno and Mitsuo Oshimura (Uno et al., 2017). A.M.T. was funded by a grant from Uniting Against Lung Cancer and is an American Cancer Society postdoctoral fellow. M.M. acknowledges support from the National Cancer Institute (1R35CA197568) and the Norman R. Seaman Endowment fund. M.M. is an American Cancer Society Research Professor.

Secondary author list

Amy Blum, Samantha J. Caesar-Johnson, John A. Demchok, Ina Felau, Melpomeni Kasapi, Martin L. Ferguson, Carolyn M. Hutter, Heidi J. Sofia, Roy Tarnuzzer, Peggy Wang, Zhining Wang, Liming Yang, Jean C. Zenklusen, Jiashan (Julia) Zhang, Sudha Chudamani, Jia Liu, Laxmi Lolla, Rashi Naresh, Todd Pihl, Qiang Sun, Yunhu Wan, Ye Wu, Juok Cho, Timothy

DeFreitas, Scott Frazer, Nils Gehlenborg, Gad Getz, David I. Heiman, Jaegil Kim, Michael S. Lawrence, Pei Lin, Sam Meier, Michael S. Noble, Gordon Saksena, Doug Voet, Hailei Zhang, Brady Bernard, Nyasha Chambwe, Varsha Dhankani, Theo Knijnenburg, Roger Kramer, Kalle Leinonen, Yuexin Liu, Michael Miller, Sheila Reynolds, Ilya Shmulevich, Vesteinn Thorsson, Wei Zhang, Rehan Akbani, Bradley M. Broom, Apurva M. Hegde, Zhenlin Ju, Rupa S. Kanchi, Anil Korkut, Jun Li, Han Liang, Shiyun Ling, Wenbin Liu, Yiling Lu, Gordon B. Mills, Kwok-Shing Ng, Arvind Rao, Michael Ryan, Jing Wang, John N. Weinstein, Jiexin Zhang, Adam Abeshouse, Joshua Armenia, Debyani Chakravarty, Walid K. Chatila, Ino de Bruijn, Jianjiong Gao, Benjamin E. Gross, Zachary J. Heins, Ritika Kundra, Konnor La, Marc Ladanyi, Augustin Luna, Moriah G. Nissan, Angelica Ochoa, Sarah M. Phillips, Ed Reznik, Francisco Sanchez-Vega, Chris Sander, Nikolaus Schultz, Robert Sheridan, S. Onur Sumer, Yichao Sun, Barry S. Taylor, Jioajiao Wang, Hongxin Zhang, Pavana Anur, Myron Peto, Paul Spellman, Christopher Benz, Joshua M. Stuart, Christopher K. Wong, Christina Yau, D. Neil Hayes, Joel S. Parker, Matthew D. Wilkerson, Adrian Ally, Miruna Balasundaram, Reanne Bowlby, Denise Brooks, Rebecca Carlsen, Eric Chuah, Noreen Dhalla, Robert Holt, Steven J.M. Jones, Katayoon Kasaian, Darlene Lee, Yussanne Ma, Marco A. Marra, Michael Mayo, Richard A. Moore, Andrew J. Mungall, Karen Mungall, A. Gordon Robertson, Sara Sadeghi, Jacqueline E. Schein, Payal Sipahimalani, Angela Tam, Nina Thiessen, Kane Tse, Tina Wong, Ashton C. Berger, Rameen Beroukhim, Andrew D. Cherniack, Carrie Cibulskis, Stacey B. Gabriel, Galen F. Gao, Gavin Ha, Matthew Meyerson, Steven E. Schumacher, Juliann Shih, Melanie H. Kucherlapati, Raju S. Kucherlapati, Stephen Baylin, Leslie Cope, Ludmila Danilova, Moiz S. Bootwalla, Phillip H. Lai, Dennis T. Maglinte, David J. Van Den Berg, Daniel J. Weisenberger, J. Todd Auman, Saianand Balu, Tom Bodenheimer, Cheng Fan, Katherine A. Hoadley, Alan P. Hoyle, Stuart R. Jefferys, Corbin D. Jones, Shaowu Meng, Piotr A. Mieczkowski, Lisle E. Mose, Amy H. Perou, Charles M. Perou, Jeffrey Roach, Yan Shi, Janae V. Simons, Tara Skelly, Matthew G. Soloway, Donghui Tan, Umadevi Veluvolu, Huihui Fan, Toshinori Hinoue, Peter W. Laird, Hui Shen, Wanding Zhou, Michelle Bellair, Kyle Chang, Kyle Covington, Chad J. Creighton, Huyen Dinh, HarshaVardhan Doddapaneni, Lawrence A. Donehower, Jennifer Drummond, Richard A. Gibbs, Robert Glenn, Walker Hale, Yi Han, Jianhong Hu, Viktoriya Korchina, Sandra Lee, Lora Lewis, Wei Li, Xiuping Liu, Margaret Morgan, Donna Morton, Donna Muzny, Jireh Santibanez, Margi Sheth, Eve Shinbrot, Linghua Wang, Min Wang, David A. Wheeler, Liu Xi, Fengmei Zhao, Julian Hess, Elizabeth L. Appelbaum, Matthew Bailey, Matthew G. Cordes, Li Ding, Catrina C. Fronick, Lucinda A. Fulton, Robert S. Fulton, Cyriac Kandoth, Elaine R. Mardis, Michael D. McLellan, Christopher A. Miller, Heather K. Schmidt, Richard K. Wilson, Daniel Crain, Erin Curley, Johanna Gardner, Kevin Lau, David Mallery, Scott Morris, Joseph Paulauskis, Robert Penny, Candace Shelton, Troy Shelton, Mark Sherman, Eric Thompson, Peggy Yena, Jay Bowen, Julie M. Gastier-Foster, Mark Gerken, Kristen M. Leraas, Tara M. Lichtenberg, Nilsa C. Ramirez, Lisa Wise, Erik Zmuda, Niall Corcoran, Tony Costello, Christopher Hovens, Andre L. Carvalho, Ana C. de Carvalho, José H. Fregnani, Adhemar Longatto-Filho, Rui M. Reis, Cristovam Scapulatempo-Neto, Henrique C.S. Silveira, Daniel O. Vidal, Andrew Burnette, Jennifer Eschbacher, Beth Hermes, Ardene Noss, Rosy Singh, Matthew L. Anderson, Patricia D. Castro, Michael Ittmann, David Huntsman, Bernard Kohl, Xuan Le, Richard Thorp, Chris Andry, Elizabeth R. Duffy,

Vladimir Lyadov, Oxana Paklina, Galiya Setdikova, Alexey Shabunin, Mikhail Tavobilov, Christopher McPherson, Ronald Warnick, Ross Berkowitz, Daniel Cramer, Colleen Feltmate, Neil Horowitz, Adam Kibel, Michael Muto, Chandrajit P. Raut, Andrei Malykh, Jill S. Barnholtz-Sloan, Wendi Barrett, Karen Devine, Jordonna Fulop, Quinn T. Ostrom, Kristen Shimmel, Yingli Wolinsky, Andrew E. Sloan, Agostino De Rose, Felice Giuliante, Marc Goodman, Beth Y. Karlan, Curt H. Hagedorn, John Eckman, Jodi Harr, Jerome Myers, Kelinda Tucker, Leigh Anne Zach, Brenda Deyarmin, Hai Hu, Leonid Kvecher, Caroline Larson, Richard J. Mural, Stella Somiari, Ales Vicha, Tomas Zelinka, Joseph Bennett, Mary Iacocca, Brenda Rabeno, Patricia Swanson, Mathieu Latour, Louis Lacombe, Bernard Têtu, Alain Bergeron, Mary McGraw, Susan M. Staugaitis, John Chabot, Hanina Hibshoosh, Antonia Sepulveda, Tao Su, Timothy Wang, Olga Potapova, Olga Voronina, Laurence Desjardins, Odette Mariani, Sergio Roman-Roman, Xavier Sastre, Marc-Henri Stern, Feixiong Cheng, Sabina Signoretti, Andrew Berchuck, Darell Bigner, Eric Lipp, Jeffrey Marks, Shannon McCall, Roger McLendon, Angeles Secord, Alexis Sharp, Madhusmita Behera, Daniel J. Brat, Amy Chen, Keith Delman, Seth Force, Fadlo Khuri, Kelly Magliocca, Shishir Maithel, Jeffrey J. Olson, Taofeek Owonikoko, Alan Pickens, Suresh Ramalingam, Dong M. Shin, Gabriel Sica, Erwin G. Van Meir, Hongzheng Zhang, Wil Eijckenboom, Ad Gillis, Esther Korpershoek, Leendert Looijenga, Wolter Oosterhuis, Hans Stoop, Kim E. van Kessel, Ellen C. Zwarthoff, Chiara Calatozzolo, Lucia Cuppini, Stefania Cuzzubbo, Francesco DiMeco, Gaetano Finocchiaro, Luca Mattei, Alessandro Perin, Bianca Pollo, Chu Chen, John Houck, Pawadee Lohavanichbutr, Arndt Hartmann, Christine Stoehr, Robert Stoehr, Helge Taubert, Sven Wach, Bernd Wullich, Witold Kycler, Dawid Murawa, Maciej Wiznerowicz, Ki Chung, W. Jeffrey Edenfield, Julie Martin, Eric Baudin, Glenn Bubley, Raphael Bueno, Assunta De Rienzo, William G. Richards, Steven Kalkanis, Tom Mikkelsen, Houtan Noushmehr, Lisa Scarpace, Nicolas Girard, Marta Aymerich, Elias Campo, Eva Giné, Armando López Guillermo, Nguyen Van Bang, Phan Thi Hanh, Bui Duc Phu, Yufang Tang, Howard Colman, Kimberley Evason, Peter R. Dottino, John A. Martignetti, Hani Gabra, Hartmut Juhl, Teniola Akeredolu, Serghei Stepa, Dave Hoon, Keunsoo Ahn, Koo Jeong Kang, Felix Beuschlein, Anne Breggia, Michael Birrer, Debra Bell, Mitesh Borad, Alan H. Bryce, Erik Castle, Vishal Chandan, John Cheville, John A. Copland, Michael Farnell, Thomas Flotte, Nasra Giama, Thai Ho, Michael Kendrick, Jean-Pierre Kocher, Karla Kopp, Catherine Moser, David Nagorney, Daniel O’Brien, Brian Patrick O’Neill, Tushar Patel, Gloria Petersen, Florencia Que, Michael Rivera, Lewis Roberts, Robert Smallridge, Thomas Smyrk, Melissa Stanton, R. Houston Thompson, Michael Torbenson, Ju Dong Yang, Lizhi Zhang, Fadi Brimo, Jaffer A. Ajani, Ana Maria Angulo Gonzalez, Carmen Behrens, Jolanta Bondaruk, Russell Broaddus, Bogdan Czerniak, Bita Esmaeli, Junya Fujimoto, Jeffrey Gershenwald, Charles Guo, Alexander J. Lazar, Christopher Logothetis, Funda Meric-Bernstam, Cesar Moran, Lois Ramondetta, David Rice, Anil Sood, Pheroze Tamboli, Timothy Thompson, Patricia Troncoso, Anne Tsao, Ignacio Wistuba, Candace Carter, Lauren Haydu, Peter Hersey, Valerie Jakrot, Hojabr Kakavand, Richard Kefford, Kenneth Lee, Georgina Long, Graham Mann, Michael Quinn, Robyn Saw, Richard Scolyer, Kerwin Shannon, Andrew Spillane, Jonathan Stretch, Maria Synott, John Thompson, James Wilmott, Hikmat Al-Ahmadie, Timothy A. Chan, Ronald Ghossein, Anuradha Gopalan, Douglas A. Levine, Victor Reuter, Samuel Singer, Bhuvanesh Singh, Nguyen Viet Tien, Thomas Broudy, Cyrus Mirsaidi, Praveen Nair, Paul Drwiega,

Judy Miller, Jennifer Smith, Howard Zaren, Joong-Won Park, Nguyen Phi Hung, Electron Kebebew, W. Marston Linehan, Adam R. Metwalli, Karel Pacak, Peter A. Pinto, Mark Schiffman, Laura S. Schmidt, Cathy D. Vocke, Nicolas Wentzensen, Robert Worrell, Hannah Yang, Marc Moncrieff, Chandra Goparaju, Jonathan Melamed, Harvey Pass, Natalia Botnariuc, Irina Caraman, Mircea Cernat, Inga Chemencedji, Adrian Clipca, Serghei Doruc, Ghenadie Gorincioi, Sergiu Mura, Maria Pirtac, Irina Stancul, Diana Tcaciuc, Monique Albert, Iakovina Alexopoulou, Angel Arnaout, John Bartlett, Jay Engel, Sebastien Gilbert, Jeremy Parfitt, Harman Sekhon, George Thomas, Doris M. Rassl, Robert C. Rintoul, Carlo Bifulco, Raina Tamakawa, Walter Urba, Nicholas Hayward, Henri Timmers, Anna Antenucci, Francesco Facciolo, Gianluca Grazi, Mirella Marino, Roberta Merola, Ronald de Krijger, Anne-Paule Gimenez-Roqueplo, Alain Piché, Simone Chevalier, Ginette McKercher, Kivanc Birsoy, Gene Barnett, Cathy Brewer, Carol Farver, Theresa Naska, Nathan A. Pennell, Daniel Raymond, Cathy Schilero, Kathy Smolenski, Felicia Williams, Carl Morrison, Jeffrey A. Borgia, Michael J. Liptay, Mark Pool, Christopher W. Seder, Kerstin Junker, Larsson Omberg, Mikhail Dinkin, George Manikhas, Domenico Alvaro, Maria Consiglia Bragazzi, Vincenzo Cardinale, Guido Carpino, Eugenio Gaudio, David Chesla, Sandra Cottingham, Michael Dubina, Fedor Moiseenko, Renumathy Dhanasekaran, Karl-Friedrich Becker, Klaus-Peter Janssen, Julia Slotta-Huspenina, Mohamed H. Abdel-Rahman, Dina Aziz, Sue Bell, Colleen M. Cebulla, Amy Davis, Rebecca Duell, J. Bradley Elder, Joe Hilty, Bahavna Kumar, James Lang, Norman L. Lehman, Randy Mandt, Phuong Nguyen, Robert Pilarski, Karan Rai, Lynn Schoenfield, Kelly Senecal, Paul Wakely, Paul Hansen, Ronald Lechan, James Powers, Arthur Tischler, William E. Grizzle, Katherine C. Sexton, Alison Kastl, Joel Henderson, Sima Porten, Jens Waldmann, Martin Fassnacht, Sylvia L. Asa, Dirk Schadendorf, Marta Couce, Markus Graefen, Hartwig Huland, Guido Sauter, Thorsten Schlomm, Ronald Simon, Pierre Tennstedt, Oluwole Olabode, Mark Nelson, Oliver Bathe, Peter R. Carroll, June M. Chan, Philip Disaia, Pat Glenn, Robin K. Kelley, Charles N. Landen, Joanna Phillips, Michael Prados, Jeff Simko, Jeffry Simko, Karen Smith-McCune, Scott VandenBerg, Kevin Roggin, Ashley Fehrenbach, Ady Kendler, Suzanne Sifri, Ruth Steele, Antonio Jimeno, Francis Carey, Ian Forgie, Massimo Mannelli, Michael Carney, Brenda Hernandez, Benito Campos, Christel Herold-Mende, Christin Jungk, Andreas Unterberg, Andreas von Deimling, Aaron Bossler, Joseph Galbraith, Laura Jacobus, Michael Knudson, Tina Knutson, Deqin Ma, Mohammed Milhem, Rita Sigmund, Andrew K. Godwin, Rashna Madan, Howard G. Rosenthal, Clement Adebamowo, Sally N. Adebamowo, Alex Boussioutas, David Beer, Thomas Giordano, Anne-Marie Mes-Masson, Fred Saad, Therese Bocklage, Lisa Landrum, Robert Mannel, Kathleen Moore, Katherine Moxley, Russel Postier, Joan Walker, Rosemary Zuna, Michael Feldman, Federico Valdivieso, Rajiv Dhir, James Luketich, Edna M. Mora Pinero, Mario Quintero-Aguilo, Carlos Gilberto Carlotti, Jr., Jose Sebastião Dos Santos, Rafael Kemp, Ajith Sankarankuty, Daniela Tirapelli, James Catto, Kathy Agnew, Elizabeth Swisher, Jenette Creaney, Bruce Robinson, Carl Simon Shelley, Eryn M. Godwin, Sara Kendall, Cassaundra Shipman, Carol Bradford, Thomas Carey, Andrea Haddad, Jeffey Moyer, Lisa Peterson, Mark Prince, Laura Rozek, Gregory Wolf, Rayleen Bowman, Kwun M. Fong, Ian Yang, Robert Korst, W. Kimryn Rathmell, J. Leigh Fantacone-Campbell, Jeffrey A. Hooke, Albert J. Kovatich, Craig D. Shriver, John DiPersio, Bettina Drake, Ramaswamy Govindan, Sharon Heath, Timothy Ley, Brian Van Tine, Peter Westervelt, Mark A. Rubin, Jung Il Lee, Natália D. Aredes,

Armaz Mariamidze, Anant Agrawal, Jaeil Ahn, Jordan Aissiou, Dimitris Anastassiou, Jesper B. Andersen, Jurandyr M. Andrade, Marco Antoniotti, Jon C. Aster, Donald Ayer, Matthew H. Bailey, Rohan Bareja, Adam J. Bass, Azfar Basunia, Oliver F. Bathe, Rebecca Batiste, Oliver Bear Don't Walk, Davide Bedognetti, Gloria Bertoli, Denis Bertrand, Bhavneet Bhinder, Gianluca Bontempi, Dante Bortone, Donald P. Bottaro, Paul Boutros, Kevin Brennan, Chaya Brodie, Scott Brown, Susan Bullman, Silvia Buonamici, Tomasz Burzykowski, Lauren Averett Byers, Fernando Camargo, Joshua D. Campbell, Francisco J. Candido dos Reis, Shaolong Cao, Maria Cardenas, Helio H.A. Carrara, Isabella Castiglioni, Anavaleria Castro, Claudia Cava, Michele Ceccarelli, Shengjie Chai, Kridsadakorn Chaichoompu, Matthew T. Chang, Han Chen, Haoran Chen, Hu Chen, Jian Chen, Jianhong Chen, Ken Chen, Ting-Wen Chen, Zhong Chen, Zhongyuan Chen, Hui Cheng, Hua-Sheng Chiu, Cai Chunhui, Giovanni Ciriello, Cristian Coarfa, Antonio Colaprico, Lee Cooper, Daniel Cui Zhou, Aedin C. Culhane, Christina Curtis, Patrycja Czerwi3ska, Aditya Deshpande, Lixia Diao, Michael Dill, Di Du, Charles G. Eberhart, James A. Eddy, Robert N. Eisenman, Mohammed Elanbari, Olivier Elemento, Kyle Ellrott, Manel Esteller, Farshad Farshidfar, Bin Feng, Camila Ferreira de Souza, Esla R. Flores, Steven Foltz, Mitchell T. Frederick, Qingsong Gao, Carl M. Gay, Zhongqi Ge, Andrew J. Gentles, Olivier Gevaert, David L. Gibbs, Adam Godzik, Abel Gonzalez-Perez, Marc T. Goodman, Dmitry A. Gordenin, Carla Grandori, Alex Graudenzi, Casey Greene, Justin Guinney, Margaret L. Gulley, Preethi H. Gunaratne, A. Ari Hakimi, Peter Hammerman, Leng Han, Holger Heyn, Le Hou, Donglei Hu, Kuan-lin Huang, Joerg Huelsken, Scott Huntsman, Peter Hurlin, Matthias Hüser, Antonio Iavarone, Marcin Imielinski, Mirazul Islam, Jacek Jassem, Peilin Jia, Cigall Kadoch, Andre Kahles, Benny Kaipparettu, Bozena Kaminska, Havish Kantheti, Rachel Karchin, Mostafa Karimi, Ekta Khurana, Pora Kim, Leszek J. Klimczak, Jia Yu Koh, Alexander Krasnitz, Nicole Kuderer, Tahsin Kurc, David J. Kwiatkowski, Teresa Laguna, Martin Lang, Anna Lasorella, Thuc D. Le, Adrian V. Lee, Ju-Seog Lee, Steve Lefever, Kjong Lehmann, Jake Leighton, Chunyan Li, Lei Li, Shulin Li, David Liu, Eric Minwei Liu, Jianfang Liu, Rongjie Liu, Yang Liu, William J.R. Longabaugh, Nuria Lopez-Bigas, Li Ma, Wencai Ma, Karen MacKenzie, Andrzej Mackiewicz, Dejan Maglic, Raunaq Malhotra, Tathiane M. Malta, Calena Marchand, R. Jay Mashl, Sylwia Mazurek, Pieter Mestdagh, Chase Miller, Marco Mina, Lopa Mishra, Younes Mokrab, Raymond Monnat, Jr., Nate Moore, Nathanael Moore, Loris Mularoni, Niranjan Nagarajan, Aaron M. Newman, Vu Nguyen, Michael L. Nickerson, Akinyemi I. Ojesina, Catharina Olsen, Sandra Orsulic, Tai-Hsien Ou Yang, James Palacino, Yinghong Pan, Elena Papaleo, Sagar Patil, Chandra Sekhar Pedamallu, Shouyong Peng, Xinxin Peng, Arjun Pennathur, Curtis R. Pickering, Christopher L. Plaisier, Laila Poisson, Eduard Porta-Pardo, Marcos Prunello, John L. Pulice, Charles Rabkin, Janet S. Rader, Kimal Rajapakshe, Aruna Ramachandran, Shuyun Rao, Xiayu Rao, Benjamin J. Raphael, Gunnar Rätsch, Brendan Reardon, Christopher J. Ricketts, Jason Roszik, Carlota Rubio-Perez, Ryan Russell, Anil Rustgi, Russell Ryan, Mohamad Saad, Thais Sabedot, Joel Saltz, Dimitris Samaras, Franz X. Schaub, Barbara G. Schneider, Adam Scott, Michael Seiler, Sara Selitsky, Sohini Sengupta, Jose A. Seoane, Jonathan S. Serody, Reid Shaw, Yang Shen, Tiago Silva, Pankaj Singh, I.K. Ashok Sivakumar, Christof Smith, Artem Sokolov, Junyan Song, Pavel Sumazin, Yutong Sun, Chayaporn Suphavilai, Najeeb Syed, David Tamborero, Alison M. Taylor, Teng Teng, Daniel G. Tiezzi, Collin Tokheim, Nora Toussaint, Mihir Trivedi, Kenneth T. Tsai, Aaron D. Tward, Eliezer Van Allen, John S.

Van Arnam, Kristel Van Steen, Carter Van Waes, Christopher P. Vellano, Benjamin Vincent, Nam S. Vo, Vonn Walter, Chen Wang, Fang Wang, Jiayin Wang, Sophia Wang, Wenyi Wang, Yue Wang, Yumeng Wang, Zehua Wang, Zeya Wang, Zixing Wang, Gregory Way, Amila Weerasinghe, Michael Wells, Michael C. Wendl, Cecilia Williams, Joseph Willis, Denise Wolf, Karen Wong, Yonghong Xiao, Lu Xinghua, Bo Yang, Da Yang, Liuqing Yang, Kai Ye, Hiroyuki Yoshida, Lihua Yu, Sobia Zaidi, Huiwen Zhang, Min Zhang, Xiaoyang Zhang, Tianhao Zhao, Wei Zhao, Zhongming Zhao, Tian Zheng, Jane Zhou, Zhicheng Zhou, Hongtu Zhu, Ping Zhu, Michael T. Zimmermann, Elad Ziv, and Patrick A. Zweidler-McKay

The members of The Cancer Genome Atlas Research Network for this project are

NCI/NHGRI Project Team

Samantha J. Caesar-Johnson, John A. Demchok, Ina Felau, Melpomeni Kasapi, Martin L. Ferguson, Carolyn M. Hutter, Heidi J. Sofia, Roy Tarnuzzer, Zhining Wang, Liming Yang, Jean C. Zenklusen, Jiashan (Julia) Zhang

TCGA DCC

Sudha Chudamani, Jia Liu, Laxmi Lolla, Rashi Naresh, Todd Pihl, Qiang Sun, Yunhu Wan, Ye Wu

Genome Data Analysis Centers (GDACs)

The Broad Institute:

Juok Cho, Timothy DeFreitas, Scott Frazer, Nils Gehlenborg, Gad Getz, David I. Heiman, Jaegil Kim, Michael S. Lawrence, Pei Lin, Sam Meier, Michael S. Noble, Gordon Saksena, Doug Voet, Hailei Zhang

Institute for Systems Biology:

Brady Bernard, Nyasha Chambwe, Varsha Dhankani, Theo Knijnenburg, Roger Kramer, Kalle Leinonen, Yuexin Liu, Michael Miller, Sheila Reynolds, Ilya Shmulevich, Vesteinn Thorsson, Wei Zhang

MD Anderson Cancer Center:

Rehan Akbani, Bradley M. Broom, Apurva M. Hegde, Zhenlin Ju, Rupa S. Kanchi, Anil Korkut, Jun Li, Han Liang, Shiyun Ling, Wenbin Liu, Yiling Lu, Gordon B. Mills, Kwok-Shing Ng, Arvind Rao, Michael Ryan, Jing Wang, John N. Weinstein, Jiexin Zhang

Memorial Sloan Kettering Cancer Center:

Adam Abeshouse, Joshua Armenia, Debyani Chakravarty, Walid K. Chatila, Ino de Bruijn, Jianjiong Gao, Benjamin E. Gross, Zachary J. Heins, Ritika Kundra, Konnor La, Marc Ladanyi, Augustin Luna, Moriah G. Nissan, Angelica Ochoa, Sarah M. Phillips, Ed Reznik,

Francisco Sanchez-Vega, Chris Sander, Nikolaus Schultz, Robert Sheridan, S. Onur Sumer, Yichao Sun, Yichao Sun, Barry S. Taylor, Jioajiao Wang, Hongxin Zhang

Oregon Health and Science University:

Pavana Anur, Myron Peto, Paul Spellman

University of California Santa Cruz:

Christopher Benz, Joshua M. Stuart, Christopher K. Wong, Christina Yau

University of North Carolina at Chapel Hill:

D. Neil Hayes, Joel S. Parker, Matthew D. Wilkerson

Genome Characterization Centers (GCC)

BC Cancer Agency:

Adrian Ally, Miruna Balasundaram, Reanne Bowlby, Denise Brooks, Rebecca Carlsen, Eric Chuah, Noreen Dhalla, Robert Holt, Steven J.M. Jones, Katayoon Kasaian, Darlene Lee, Yussanne Ma, Marco A. Marra, Michael Mayo, Richard A. Moore, Andrew J. Mungall, Karen Mungall, A. Gordon Robertson, Sara Sadeghi, Jacqueline E. Schein, Payal Sipahimalani, Angela Tam, Nina Thiessen, Kane Tse, Tina Wong

The Broad Institute:

Ashton C. Berger, Rameen Beroukhim, Andrew D. Cherniack, Carrie Cibulskis, Stacey B. Gabriel, Galen F. Gao, Gavin Ha, Matthew Meyerson, Gordon Saksena, Steven E. Schumacher, Juliann Shih

Harvard:

Melanie H. Kucherlapati, Raju S. Kucherlapati

Johns Hopkins:

Stephen Baylin, Leslie Cope, Ludmila Danilova

University of Southern California:

Moiz S. Bootwalla, Phillip H. Lai, Dennis T. Maglinte, David J. Van Den Berg, Daniel J. Weisenberger

University of North Carolina at Chapel Hill:

J. Todd Auman, Saianand Balu, Tom Bodenheimer, Cheng Fan, D. Neil Hayes, Katherine A. Hoadley, Alan P. Hoyle, Stuart R. Jefferys, Corbin D. Jones, Shaowu Meng, Piotr A. Mieczkowski, Lisle E. Mose, Joel S. Parker, Amy H. Perou, Charles M. Perou, Jeffrey

Roach, Yan Shi, Janae V. Simons, Tara Skelly, Matthew G. Soloway, Donghui Tan, Umadevi Veluvolu, Matthew D. Wilkerson

Van Andel Research Institute:

Huihui Fan, Toshinori Hinoue, Peter W. Laird, Hui Shen, Wanding Zhou

Genome Sequencing Centers (GSC)

Baylor College of Medicine:

Michelle Bellair, Kyle Chang, Kyle Covington, Chad J. Creighton, Huyen Dinh, HarshaVardhan Doddapaneni, Lawrence A. Donehower, Jennifer Drummond, Richard A. Gibbs, Robert Glenn, Walker Hale, Yi Han, Jianhong Hu, Viktoriya Korchina, Sandra Lee, Lora Lewis, Wei Li, Xiuping Liu, Margaret Morgan, Donna Morton, Donna Muzny, Jireh Santibanez, Margi Sheth, Eve Shinbrot, Linghua Wang, Min Wang, David A. Wheeler, Liu Xi, Fengmei Zhao

The Broad Institute:

Carrie Cibulskis, Stacy B. Gabriel, Julian Hess

Washington University at St. Louis:

Elizabeth L. Appelbaum, Matthew Bailey, Matthew G. Cordes, Li Ding, Catrina C. Fronick, Lucinda A. Fulton, Robert S. Fulton, Cyriac Kandoth, Elaine R. Mardis, Michael D. McLellan, Christopher A. Miller, Heather K. Schmidt, Richard K. Wilson

Bio specimen Core Resource

The International Genomics Consortium:

Daniel Crain, Erin Curley, Johanna Gardner, Kevin Lau, David Mallery, Scott Morris, Joseph Paulauskis, Robert Penny, Candace Shelton, Troy Shelton, Mark Sherman, Eric Thompson, Peggy Yena

Nationwide Children’s Organization:

Jay Bowen, Julie M. Gastier-Foster, Mark Gerken, Kristen M. Leraas, Tara M. Lichtenberg, Nilsa C. Ramirez, Lisa Wise, Erik Zmuda

Tissue Source Sites

Australian Prostate Cancer Research Center:

Niall Corcoran, Tony Costello, Christopher Hovens

Barretos Cancer Hospital:

Andre L. Carvalho, Ana C. de Carvalho, Jose H. Fregnani, Adhemar Longatto-Filho, Rui M. Reis, Cristovam Scapulatempo-Neto, Henrique C. S. Silveira, Daniel O. Vidal

Barrow Neurological Institute:

Andrew Burnette, Jennifer Eschbacher, Beth Hermes, Ardene Noss, Rosy Singh

Baylor College of Medicine:

Matthew L. Anderson, Patricia D. Castro, Michael Ittmann

BC Cancer Agency:

David Huntsman

BioreclamationIVT:

Bernard Kohl, Xuan Le, Richard Thorp

Boston Medical Center:

Chris Andry, Elizabeth R. Duffy

Botkin Hospital:

Vladimir Lyadov, Oxana Paklina, Galiya Setdikova, Alexey Shabunin, Mikhail Tavobilov

Brain Tumor Center at the University of Cincinnati Gardner Neuroscience Institute:

Christopher McPherson, Ronald Warnick

Brigham and Women's Hospital:

Ross Berkowitz, Daniel Cramer, Colleen Feltmate, Neil Horowitz, Adam Kibel, Michael Muto, Chandrajit P. Raut

Capital Biosciences, Inc.:

Andrei Malykh

Case Comprehensive Cancer Center:

Jill S. Barnholtz-Sloan, Wendi Barrett, Karen Devine, Jordonna Fulop, Quinn T. Ostrom, Kristen Shimmel, Yingli Wolinsky

Case Western Reserve School of Medicine:

Andrew E. Sloan

Catholic University of the Sacred Heart:

Agostino De Rose, Felice Giuliante

Cedars-Sinai Medical Center:

Marc Goodman, Beth Y. Karlan

Central Arkansas Veterans Healthcare System:

Curt H. Hagedorn

Centura Health:

John Eckman, Jodi Harr, Jerome Myers, Kelinda Tucker, Leigh Anne Zach

Chan Soon-Shiong Institute of Molecular Medicine at Windber:

Brenda Deyarmin, Hai Hu, Leonid Kvecher, Caroline Larson, Richard J. Mural, Stella Somiari

Charles University:

Ales Vicha, Tomas Zelinka

Christiana Care Health System:

Joseph Bennett, Mary Iacocca, Brenda Rabeno, Patricia Swanson

CHU of Montreal:

Mathieu Latour

CHU of Quebec:

Louis Lacombe, Bernard Tetu

CHU of Quebec, Laval University Research Center of Chus:

Alain Bergeron

Cleveland Clinic Foundation:

Mary McGraw, Susan M. Staugaitis

Columbia University:

John Chabot, Hanina Hibshoosh, Antonia Sepulveda, Tao Su, Timothy Wang

Cureline, Inc.:

Olga Potapova, Olga Voronina

Curie Institute:

Laurence Desjardins, Odette Mariani, Sergio Roman-Roman, Xavier Sastre, Marc-Henri Stern

Dana-Farber Cancer Institute:

Feixiong Cheng, Sabina Signoretti

Dignity Health Mercy Gilbert Medical Center:

Jennifer Eschbacher

Duke University Medical Center:

Andrew Berchuck, Darell Bigner, Eric Lipp, Jeffrey Marks, Shannon McCall, Roger McLendon, Angeles Secord, Alexis Sharp

Emory University:

Madhusmita Behera, Daniel J. Brat, Amy Chen, Keith Delman, Seth Force, Fadlo Khuri, Fadlo Khuri, Kelly Magliocca, Shishir Maithel, Jeffrey J. Olson, Taofeek Owonikoko, Alan Pickens, Suresh Ramalingam, Dong M. Shin, Gabriel Sica, Gabriel Sica, Erwin G. Van Meir, Erwin G. Van Meir, Hongzheng Zhang

Erasmus Medical Center:

Wil Eijckenboom, Ad Gillis, Esther Korpershoek, Leendert Looijenga, Wolter Oosterhuis, Hans Stoop, Kim E. van Kessel, Ellen C. Zwarthoff

Foundation of the Carlo Besta Neurological Institute, IRCCS:

Chiara Calatozzolo, Lucia Cuppini, Stefania Cuzzubbo, Francesco DiMeco, Gaetano Finocchiaro, Luca Mattei, Alessandro Perin, Bianca Pollo

Fred Hutchinson Cancer Research Center:

Chu Chen, John Houck, Pawadee Lohavanichbutr

Friedrich-Alexander-University:

Arndt Hartmann, Christine Stoehr, Robert Stoehr, Helge Taubert, Sven Wach, Bernd Wullich

Greater Poland Cancer Center:

Witold Kycler, Dawid Murawa, Maciej Wiznerowicz

Greenville Health System Institute for Translational Oncology Research:

Ki Chung, W. Jeffrey Edenfield, Julie Martin

Gustave Roussy institute:

Eric Baudin

Harvard University:

Glenn Bubley, Raphael Bueno, Assunta De Rienzo, William G. Richards

Henry Ford Health System:

Ana deCarvalho, Steven Kalkanis, Tom Mikkelsen, Tom Mikkelsen, Houtan Noushmehr, Lisa Scarpace

Hospices Civils de Lyon:

Nicolas Girard

Hospital Clinic:

Marta Aymerich, Elias Campo, Eva Gine, Armando Lopez Guillermo

Hue Central Hospital:

Nguyen Van Bang, Phan Thi Hanh, Bui Duc Phu

Human Tissue Resource Network:

Yufang Tang

Huntsman Cancer Institute:

Howard Colman, Kimberley Evason

Icahn School of Medicine at Mount Sinai:

Peter R. Dottino, John A. Martignetti

Imperial College London:

Hani Gabra

Indivumed GmbH:

Hartmut Juhl

Institute of Human Virology Nigeria:

Teniola Akeredolu

Institute of Urgent Medicine:

Serghei Stepa

John Wayne Cancer Institute:

Dave Hoon

Keimyung University:

Keunsoo Ahn, Koo Jeong Kang

Ludwich Maximilians University Munich:

Felix Beuschlein

Maine Medical Center:

Anne Breggia

Massachusetts General Hospital:

Michael Birrer

Mayo Clinic:

Debra Bell, Mitesh Borad, Alan H. Bryce, Erik Castle, Vishal Chandan, John Cheville, John A. Copland, Michael Farnell, Thomas Flotte, Nasra Giama, Thai Ho, Michael Kendrick, Jean-Pierre Kocher, Karla Kopp, Catherine Moser, David Nagorney, Daniel O'Brien, Brian Patrick O'Neill, Tushar Patel, Gloria Petersen, Gloria Petersen, Florencia Que, Michael Rivera, Lewis Roberts, Robert Smallridge, Robert Smallridge, Thomas Smyrk, Thomas Smyrk, Melissa Stanton, R. Houston Thompson, Michael Torbenson, Ju Dong Yang, Lizhi Zhang, Lizhi Zhang

McGill University Health Center:

Fadi Brimo

MD Anderson Cancer Center:

Jaffer A. Ajani, Ana Maria Angulo Gonzalez, Carmen Behrens, Jolanta Bondaruk, Russell Broaddus, Bradley Broom, Bogdan Czerniak, Bita Esmaeli, Junya Fujimoto, Jeffrey Gershenwald, Charles Guo, Alexander J. Lazar, Christopher Logothetis, Funda Meric-Bernstam, Funda Meric-Bernstam, Cesar Moran, Lois Ramondetta, David Rice, Anil Sood, Pheroze Tamboli, Timothy Thompson, Patricia Troncoso, Patricia Troncoso, Anne Tsao, Ignacio Wistuba

Melanoma Institute Australia:

Candace Carter, Lauren Haydu, Peter Hersey, Valerie Jakrot, Hojabr Kakavand, Richard Kefford, Kenneth Lee, Georgina Long, Graham Mann, Michael Quinn, Robyn Saw, Richard Scolyer, Kerwin Shannon, Andrew Spillane, Jonathan Stretch, Maria Synott, John Thompson, James Wilmott

Memorial Sloan Kettering Cancer Center:

Hikmat Al-Ahmadie, Timothy A. Chan, Ronald Ghossein, Anuradha Gopalan, Douglas A. Levine, Victor Reuter, Samuel Singer, Bhuvanesh Singh

Ministry of Health of Vietnam:

Nguyen Viet Tien

Molecular Response:

Thomas Broudy, Cyrus Mirsaidi, Praveen Nair

Nancy N. and J.C. Lewis Cancer & Research Pavilion at St. Joseph's/Candler:

Paul Drwiega, Judy Miller, Jennifer Smith, Howard Zaren

National Cancer Center Korea:

Joong-Won Park

National Cancer Hospital of Vietnam:

Nguyen Phi Hung

National Cancer Institute:

Electron Kebebew, W. Marston Linehan, Adam R. Metwalli, Karel Pacak, Peter A. Pinto, Mark Schiffman, Laura S. Schmidt, Cathy D. Vocke, Nicolas Wentzensen, Robert Worrell, Hannah Yang

Norfolk & Norwich University Hospital:

Marc Moncrieff

NYU Langone Medical Center:

Chandra Goparaju, Jonathan Melamed, Harvey Pass

Oncology Institute:

Natalia Botnariuc, Irina Caraman, Mircea Cernat, Inga Chemencedji, Adrian Clipca, Serghei Doruc, Ghenadie Gorincioi, Sergiu Mura, Maria Pirtac, Irina Stancul, Diana Tcaciuc

Ontario Tumour Bank:

Monique Albert, Iakovina Alexopoulou, Angel Arnaout, John Bartlett, Jay Engel, Sebastien Gilbert, Jeremy Parfitt, Harman Sekhon

Oregon Health & Science University:

George Thomas

Papworth Hospital NHS Foundation Trust:

Doris M. Rassl, Robert C. Rintoul

Providence Health and Services:

Carlo Bifulco, Raina Tamakawa, Walter Urba

QIMR Berghofer Medical Research Institute:

Nicholas Hayward

Radboud Medical University Center:

Henri Timmers

Regina Elena National Cancer Institute:

Anna Antenucci, Francesco Facciolo, Gianluca Grazi, Mirella Marino, Roberta Merola

Reinier de Graaf Hospital:

Ronald de Krijger

René Descartes University:

Anne-Paule Gimenez-Roqueplo

Research Center of Chus Sherbrooke, Québec:

Alain Piche

Research Institute of the McGill University Health Centre:

Simone Chevalier, Ginette McKercher

Rockefeller University:

Kivanc Birsoy

Rose Ella Burkhardt Brain Tumor and Neuro-Oncology Center:

Gene Barnett, Cathy Brewer, Carol Farver, Theresa Naska, Nathan A. Pennell, Daniel Raymond, Cathy Schilero, Kathy Smolenski, Felicia Williams

Roswell Park Cancer Institute:

Carl Morrison

Rush University:

Jeffrey A. Borgia, Michael J. Liptay, Mark Pool, Christopher W. Seder

Saarland University:

Kerstin Junker

Sage Bionetworks:

Larsson Omberg

Saint-Petersburg City Clinical Oncology Hospital:

Mikhail Dinkin, George Manikhas

Sapienza University of Rome:

Domenico Alvaro, Maria Consiglia Bragazzi, Vincenzo Cardinale, Guido Carpino, Eugenio Gaudio

Spectrum Health:

David Chesla, Sandra Cottingham

St. Petersburg Academic University RAS:

Michael Dubina, Fedor Moiseenko

Stanford University:

Renumathy Dhanasekaran

Technical University of Munich:

Karl-Friedrich Becker, Klaus-Peter Janssen, Julia Slotta-Huspenina

The International Genomics Consortium:

Daniel Crain, Erin Curley, Johanna Gardner, David Mallery, Scott Morris, Joseph Paulauskis, Robert Penny, Candace Shelton, Troy Shelton, Eric Thompson

The Ohio State University:

Mohamed H. Abdel-Rahman, Dina Aziz, Sue Bell, Colleen M. Cebulla, Amy Davis, Rebecca Duell, J. Bradley Elder, Joe Hilty, Bahavna Kumar, James Lang, Norman L. Lehman, Randy Mandt, Phuong Nguyen, Robert Pilarski, Karan Rai, Lynn Schoenfield, Kelly Senecal, Paul Wakely

The Oregon Clinic:

Paul Hansen

The Research Institute at Nationwide Children's Hospital:

Nilsa Ramirez

Tufts Medical Center:

Ronald Lechan, James Powers, Arthur Tischler

University of Alabama at Birmingham Medical Center:

William E. Grizzle, Katherine C. Sexton

UC Cancer Institute:

Alison Kastl

UCSF-Helen Diller Family Comprehensive Cancer Center:

Joel Henderson, Sima Porten

University Hospital of Giessen and Marburg:

Jens Waldmann

University Hospital in Wurzburg, Germany:

Martin Fassnacht

University Health Network:

Sylvia L. Asa

University Hospital Essen:

Dirk Schadendorf

University Hospitals Case Medical Center Hamburg-Eppendorf::

Marta Couce, Markus Graefen, Hartwig Huland, Guido Sauter, Thorsten Schlomm, Ronald Simon, Pierre Tennstedt

University of Abuja Teaching Hospital:

Oluwole Olabode

University of Arizona:

Mark Nelson

University of Calgary:

Oliver Bathe

University of California:

Peter R. Carroll, June M. Chan, Philip Disaia, Pat Glenn, Robin K. Kelley, Charles N. Landen, Joanna Phillips, Michael Prados, Jeff Simko, Jeffry Simko, Karen Smith-McCune, Scott VandenBerg

University of Chicago Medicine:

Kevin Roggin

University of Cincinnati:

Ashley Fehrenbach, Ady Kendler

University of Cincinnati Cancer Institute:

Suzanne Sifri, Ruth Steele

University of Colorado Cancer Center:

Antonio Jimeno

University of Dundee:

Francis Carey, Ian Forgie

University of Florence:

Massimo Mannelli

University of Hawaii Cancer Center:

Michael Carney, Brenda Hernandez

University of Heidelberg:

Benito Campos, Christel Herold-Mende, Christin Jungk, Andreas Unterberg, Andreas von Deimling

University of Iowa Hospital & Clinics:

Aaron Bossler, Joseph Galbraith, Laura Jacobus, Michael Knudson, Tina Knutson, Deqin Ma, Mohammed Milhem, Rita Sigmund

University of Kansas Medical Center:

Andrew K. Godwin, Rashna Madan, Howard G. Rosenthal

University of Maryland School of Medicine:

Clement Adebamowo, Sally N. Adebamowo

University of Melbourne:

Alex Boussioutas

University of Michigan:

David Beer, Thomas Giordano

University of Montreal:

Anne-Marie Mes-Masson, Fred Saad

University of New Mexico:

Therese Bocklage

University of Oklahoma:

Lisa Landrum, Robert Mannel, Kathleen Moore, Katherine Moxley, Russel Postier, Joan Walker, Rosemary Zuna

University of Pennsylvania:

Michael Feldman, Federico Valdivieso

University of Pittsburgh:

Rajiv Dhir, James Luketich

University of Puerto Rico:

Edna M. Mora Pinero, Mario Quintero-Aguilo

University of São Paulo:

Carlos Gilberto Carlotti Junior, Jose Sebastiao Dos Santos, Rafael Kemp, Ajith Sankarankuty, Daniela Tirapelli

University of Sheffield Western Bank:

James Catto

University of Washington:

Kathy Agnew, Elizabeth Swisher

University of Western Australia:

Jenette Creaney, Bruce Robinson

University of Wisconsin School of Medicine and Public Health:

Carl Simon Shelley

University of Kansas Cancer Center:

Eryn M. Godwin, Sara Kendall, Cassaundra Shipman

University of Michigan:

Carol Bradford, Thomas Carey, Andrea Haddad, Jeffey Moyer, Lisa Peterson, Mark Prince, Laura Rozek, Gregory Wolf

UQ Thoracic Research Centre:

Rayleen Bowman, Kwun M. Fong, Ian Yang

Valley Health System:

Robert Korst

Vanderbilt University Medical Center:

W. Kimryn Rathmell

Walter Reed National Medical Center:

J. Leigh Fantacone-Campbell, Jeffrey A. Hooke, Albert J. Kovatich, Craig D. Shriver

Washington University:

John DiPersio, Bettina Drake, Ramaswamy Govindan, Sharon Heath, Timothy Ley, Brian Van Tine, Peter Westervelt

Weill Cornell Medical College:

Mark A. Rubin

Yonsei University College of Medicine:

Jung Il Lee

Institution Not Provided:

Natalia D. Aredes, Armaz Mariamidze

Institution Addresses

Australian Prostate Cancer Research Center, Epworth Hospital, VIC, Australia

Australian Prostate Cancer Research Center, Epworth Hospital, VIC, Australia

Barretos Cancer Hospital, Av: Antenor Duarte Villela, 1331, Barretos, Sao Paulo, Brazil

Barrow Neurological Institute, St. Joseph’s Hospital and Medical Center, Phoenix, Arizona 85013

Barrow Neurological Institute, St. Joseph’s Hospital and Medical Center, Phoenix, Arizona 85013,

Baylor College of Medicine One Baylor Plaza, Houston, TX 77030

BC Cancer Agency, 675 W 10th Ave, Vancouver, BC V5Z 1L3, Canada

Beth Israel Deaconess Medical Center Harvard University Medical School Boston Mass

BioreclamationIVT, 99 Talbot Blvd Chestertown, MD 21620

Boston Medical Center, Boston MA 02118

Botkin Hospital, 2-y Botkinskiy pr-d, 5, Moskva, Russia, 125284

Brain Tumor and Neuro-oncology Center, Department of Neurosurgery, University Hospitals Case Medical Center, Case Western Reserve School of Medicine, 11100 Euclid Ave, Cleveland, Ohio, 44106

Brain Tumor Center at the University of Cincinnati Gardner Neuroscience Institute, and Department of Neurosurgery, University of Cincinnati College of Medicine, and Mayfield Clinic, 260 Stetson Street, Suite 2200, Cincinnati, Ohio, 45219

Brain Tumor Center at the University of Cincinnati Neuroscience Institute, and Department of Neurosurgery, University of Cincinnati College of Medicine, and Mayfield Clinic, 234 Goodman Street, Cincinnati, Ohio, 45219

Brigham and Women’s Hospital, 75 Francis St, Boston MA 02115

Capital Biosciences, Inc., 900 Clopper Rd, Suite 120, Gaithersburg, MD 20878

Case Comprehensive Cancer Center, 11100 Euclid Ave - Wearn 152, Cleveland, OH 44106-5065

Cedars-Sinai Medical Center, 8700 Beverly Boulevard, Suite 290 West MOT, Los Angeles, CA

Center for Liver Cancer, National Cancer Center Korea, 323 Ilsan-ro, Ilsan dong-gu, Goyang, Gyeonggi 10408, South Korea

Central Arkansas Veterans Healthcare System, Little Rock, AR 72205

CHU of Quebec, Laval University Research Center of Chus 2705, boul. Laurier Bureau TR72

QUÉBEC, Quebec G1V 4G2

Centura Health 9100 E Mineral Cir, Centennial, CO 80112

Chan Soon-Shiong Institute of Molecular Medicine at Windber, Windber, PA 15963

Charles University, Czech Republic

CHU of Quebec, Hôtel-Dieu de Quebec-University Laval, 11 cote du palais, Quebec City, G1R 2J6

CHUM, Montreal, Qc, Canada.

Clinic of Urology and Pediatric Urology, Saarland University, Homburg, Germany.

Clinical Breast Care Project, Murtha Cancer Center, Uniformed Services University / Walter Reed National Military Medical Center, Bethesda, MD 20889

Comprehensive Cancer Center Tissue Procurement Shared Resource, Cooperative Human Tissue Network

Midwestern Division, Dept. of Pathology, Human Tissue Resource Network, The Ohio State University, 410 West 10th Ave, Doan Hall, Room E413A, Columbus, OH 43210

Cureline, Inc., 290 Utah Ave, Ste 300, South san Francisco, CA 94080, USA

Dana-Farber Cancer Institute, 450 Brookline Ave, Boston MA, 02215

Dardinger Neuro-Oncology Center, Department of Neurosurgery, James Comprehensive Cancer Center and The Ohio State University Medical Center, 320 W 10th Ave, Columbus, Ohio, 43210

Department of Cardiovascular and Thoracic Surgery. Suite 774 Professional Office Building. 1735 W. Harrison St., Chicago, IL 60612

Department of Epidemiology and Public Health, University of Maryland School of Medicine, Baltimore MD 21201

Department of Genetics & Genomic Sciences, Icahn School of Medicine at Mount Sinai, 1 Gustave L. Levy Place, New York, NY 10029

Department of Hematology and Medical Oncology, Mayo Clinic Arizona, 5779 E. Mayo Blvd, Phoenix AZ 85054

Department of Medicine, University of Wisconsin School of Medicine and Public Health, 1685 Highland Avenue, Madison, WI 53705

Department of Medicine, Washington University in St. Louis, 660 S. Euclid Ave., CB 8066, St. Louis, MO 63110

Department of Medicine, Yonsei University College of Medicine, Seoul, Republic of Korea

Department of Neurological Surgery

Department of Neurosurgery, Emory University School of Medicine, 1365 Clifton Road, NE, Atlanta, GA 30322

Department of Obstetrics and Gynecology, Baylor College of Medicine, One Baylor Plaza, Houston, Texas 77030

Department of Obstetrics/Gynecology and Reproductive Sciences, Icahn School of Medicine at Mount Sinai, 1 Gustave L. Levy Place, New York, NY 10029

Department of Orthopedic Surgery, University of Kansas Medical Center 3901 Rainbow Boulevard, Kansas City, KS 66160

Department of Pathology and Cell Biology, Columbia University, New York, NY10032

Department of Pathology and Immunology, Baylor College of Medicine, One Baylor Plaza, Houston, TX 77030

Department of Pathology and Laboratory Medicine, University of Kansas Medical Center, Kansas City, KS 66206

Department of Pathology, Department of Cell and Molecular Medicine. 570 Jelke South center, 1750 W. Harrison St., Chicago, IL 60612

Department of Pathology, Duke University School of Medicine, Durham, NC 27710

Department of Pathology, Spectrum Health, 35 Michigan NE, Grand Rapids, MI 49503

Department of Pathology, The Ohio State University School of Medicine, N308 Doan Hall, 410 W 10th Ave, Columbus, OH-43210-1267

Department of Pathology, The Ohio State University Wexner Medical Center (Doan Hall N337B, 410 West 10th Ave., Columbus, OH 43210

Department of Pathology. 570 Jelke South center, 1750 W. Harrison St., Chicago, IL 60612

Department of Surgery and Anatomy, Ribeirao Preto Medical School - FMRP, University of Sao Paulo, Brazil, 14049-900

Department of Surgery and Cancer, Imperial College London, Du Cane Road London W12 0NN, UK

Department of Surgery, Brigham and Women’s Hospital, Harvard Medical School, Boston, MA, USA

Department of Surgery, Columbia University, New York, NY 10032

Department of Surgery, University of Michigan, Ann Arbor MI 48109

Department of Urology and Pediatric Urology, University Hospital Erlangen, Friedrich-Alexander-University Erlangen-Nuremberg, 91054 Erlangen, Germany

Department of Urology, Mayo Clinic Arizona, 5779 E. Mayo Blvd, Phoenix AZ 85054

Departments of Neurosurgery and Hematology and Medical Oncology, School of Medicine and Winship Cancer Institute, 1365C Clifton Rd. N.E., Emory University, Atlanta, GA 30322

Departments of Pathology & Translational Molecular Pathology, The University of Texas MD Anderson Cancer Center, 1515 Holcombe Blvd--Unit 85, Houston, Texas, USA

Dept. of Pathology & Laboratory Medicine, University of Cincinnati, UC Health University Hospital, 234 Goodman Street, Cincinnati, OH 45219-0533

Dept. of Pathology, Robert J. Tomsich Pathology & Laboratory Medicine Institute, Lerner Research Inst, Cleveland Clinic Foundation, Cleveland, OH 44195

Dept. of Surgery, Klinikum rechts der Isar, Technical University of Munich, Ismaninger Str. 22, 81675 Munich, Germany

Dignity Health Mercy Gilbert Medical Center 3555 S Val Vista Dr, Gilbert, AZ 85297

Division Molecular Urology, Department of Urology and Pediatric Urology, University Hospital Erlangen, Friedrich-Alexander-University Erlangen-Nuremberg, 91054 Erlangen, Germany

Division of Cancer Epidemiology and Genetics, National Cancer Institute, 9609 Medical Center Dr. Bethesda 20892 USA

Division of Neurosurgical Research, Dpt. Neurosurgery, University of Heidelberg, INF 400, 69120 Heidelberg, Germany

Division of Surgical Oncology, Department of Surgery, Brigham and Women’s Hospital, 75 Francis Street, Boston, MA 02115

Dpt. Neuropathology, University of Heidelberg, INF 224, 69120 Heidelberg, Germany

Dpt. Neurosurgery, University of Heidelberg, INF 400, 69120 Heidelberg, Germany

Duke University

Duke University Medical Center 177 MSRB Box 3156 Durham, NC 27710

Duke University Medical Center, Gynecologic Oncology, Box 3079, Durham, NC USA

Emory University, 1365 Clifton Road, NE Atlanta GA, 30322

Erasmus MC, Wytemaweg 80, 3015 CN, Rotterdam, The Netherlands

Erasmus Medical Center

Erasmus University Medical Center Rotterdam, Cancer Institute, Wytemaweg 80, 3015CN, Rotterdam, the Netherlands

The Foundation of the Carlo Besta Neurological Institute, IRCCS via Celoria 11, 20133

Fred Hutchinson Cancer Research Center, 1100 Fairview Ave N, Seattle, WA 98019

Greater Poland Cancer Center, Garbary 15, 61-866 Poznań Poland

Greenville Health System Institute for Translational Oncology Research 900 West Faris Road Greenville SC 29605 Harvard University Cambridge, MA 02138

Havener Eye Institute, The Ohio State University Wexner Medical Center 915 Olentangy River Rd, Columbus, OH 43212

Henry Ford Hospital 2799 West Grand Blvd Detroit MI USA 48202

Hepatobiliary Surgery Unit, A. Gemelli Hospital, Catholic University of the Sacred Heart, Largo Agostino Gemelli 8, 00168 Rome, Italy

Hermelin Brain Tumor Center, Henry Ford Health System, 2799 W Grand Blvd, Detroit, MI, 48202

Hospices Civils de Lyon, CARDIOBIOTEC, Lyon F-69677, France

Hospital Clinic, Villarroel 180, Barcelona, Spain, 08036

Hue Central Hospital, Hue, Vietnam

Human Tissue Resource Network, Dept. of Pathology, College of Medicine, 1615 Polaris Innovation Ctr, 2001 Polaris, Columbus 43240

Huntsman Cancer Institute, Univ. of Utah, 2000 Circle of Hope, Salt Lake City, UT 84112

Indivumed GmbH, 20251 Hamburg, Germany

René Descartes University, Hospital Europeen Georges Pompidou, 20 rue Leblanc, 75015, Paris, France

Curie Institute, 26 rue Ulm, 75005 Paris, France

Gustave Roussy Institute of Oncology, 39 Rue Camille Desmoulins 94805, Villejuif, France

Institute of Human Virology Nigeria, Abuja, Nigeria

Institute of Pathology, Technical University of Munich, Trogerstr. 18, 83675 Munich, Germany

Institute of Pathology, University Hospital Erlangen, Firedrich-Alexander-University Erlangen-Nuremberg, 91054 Erlangen, Germany

Institute of Urgent Medicine, Republic of Moldova

Regina Elena National Cancer Institute Irccs - Ifo, Via Elio Chianesi 53, 00144, Rome, Italy

John Wayne Cancer Institute, 2200 Santa Monica Blvd, Santa Monica, CA 90404

Keimyung University, Daegu, South Korea

Knight Comprehensive Cancer Institute, Oregon Health & Science University

Ludwich Maximilians University Munich, Ziemssenstrasse 1, D-80336, Munich, Germany

Maine Medical Center, 22 Bramhall St., Portland, ME 04102

Martini-Clinic, Prostate Cancer Center, University Medical Center Hamburg-Eppendorf, Martinistr. 52, D-20246

Hamburg, Germany

Massachusetts General Hospital 55 Fruit Street Boston Ma 02114

Mayo Clinic 5777 E Mayo Blvd, Phoenix, Arizona 85054

Mayo Clinic 4500 San Pablo Road Jacksonville, FL 32224

Mayo Clinic, 200 First St. SW, Rochester, MN 55905

Mayo Clinic, Rochester, MN 55905

McGill University Health Center. 1001 Decarie Blvd, Montreal, QC, Canada H4A 3J1

MD Anderson Cancer Center 1515 Holcombe Blvd. Unit 0085 Houston, TX 77030

MD Anderson Cancer Center, Department of Pathology, Unit 085; 1515

MD Anderson Cancer Center Life Science Plaza Building 2130 W. Holcombe Blvd, Unit 2951 Houston, TX 77030

Office: LSP9.4029

Melanoma Institute Australia, North Sydney, NSW, Australia 2060

Memorial Sloan Kettering Cancer Center Department of Pathology, 1275 York Avenue, New York, NY 10065

Memorial Sloan Kettering Cancer Center, 1275 York Avenue, New York, NY 10065

Memorial Sloan Kettering Cancer Center, Center for Molecular Oncology, 1275 York Avenue, New York, NY 10065

Ministry of Health of Vietnam, Hanoi, Vietnam

Molecular Pathology Shared Resource of Herbert Irving Comprehensive Cancer Center of Columbia University, New York, NY10032

Molecular Response 11011 Torreyana Road San Diego, CA 92121

Murtha Cancer Center, Uniformed Services University / Walter Reed National Military Medical Center, Bethesda, MD 20889

Nancy N. and J.C. Lewis Cancer & Research Pavilion at St. Joseph's/Candler, 225 Candler Drive, Savannah, GA 31405

National Cancer Hospital of Vietnam

National Cancer Institute, 31 Center Dr, Bethesda, MD 20892

National Cancer Institute, Bethesda, MD 20892

Norfolk & Norwich University Hospital, Norwich, UK. NR4 7UY

NYU Langone Medical Center, Cardiothoracic Surgery, 530 first Avenue, 9V, New York, NY

Oncology Institute, Republic of Moldova

Ontario Tumor Bank - Hamilton site, St. Joseph's Healthcare Hamilton, Hamilton, Ontario L8N 3Z5, Canada

Ontario Tumor Bank - Kingston site, Kingston General Hospital, Kingston, Ontario K7L 5H6, Canada

Ontario Tumor Bank – Ottawa site, The Ottawa Hospital, Ottawa, Ontario K1H 8L6, Canada.

Ontario Tumor Bank, London Health Sciences Centre, London, Ontario N6A 5A5, Canada

Ontario Tumor Bank, Ontario Institute for Cancer Research, Toronto, Ontario M5G 0A3, Canada

Orbital Oncology & Ophthalmic Plastic Surgery Department of Plastic Surgery M.D. Anderson Cancer Center 1515

Holcombe Blvd, Unit 1488 Houston, Texas 77030

Papworth Hospital NHS Foundation Trust, UK

Pathology, St. Joseph's/Candler, 5353 Reynolds St., Savannah, GA 31405

Professor, Division of Neuropathology, Department of Pathology, University Hospitals Case Medical Center

Program in Epidemiology, Fred Hutchinson Cancer Research Center, Seattle, WA 98109

Providence Health and Services

QIMR Berghofer Medical Research Institute, Herston, QLD, Australia

Radboud Medical University Center, Geert Grooteplein-Zuid 10, Nijmegen, the Netherlands

Regina Elena National Cancer Institute, 00144 Rome, Italy

Reinier de Graaf Hospital, Reinier de Graafweg 5, 2625AD, Delft, the Netherlands

Research Institute of the McGill University Health Centre, McGill University, Montreal, Quebec, Canada

Research Center Of Chus Sherbrooke, Quebec aile 9, porte 6, 3001 12e Avenue Nord, Sherbrooke, QC J1H 5N4, Canada

Rockefeller University 1230 York Ave New York, NY

Rose Ella Burkhardt Brain Tumor and Neuro-Oncology Center ND4-52A, Cleveland Clinic Foundation, 9500 Euclid Ave, Cleveland, OH 44195

Rose Ella Burkhardt Brain Tumor and Neuro-Oncology Center, 9500 Euclid Avenue - CA51, Cleveland, OH 44195

Rose Ella Burkhardt Brain Tumor and Neuro-Oncology Center, Department of Neurosurgery, Neurological and Taussig Cancer Institute, Cleveland Clinic, 9500 Euclid Avenue, Cleveland, Ohio, 44195

Roswell Park Cancer Institute. Elm & Carlton Streets, Buffalo NY 14263

Sage Bionetworks, Seattle, WA 98109

Saint-Petersburg City Clinical Oncology Hospital, 56 Veteranov prospect, Saint-Petersburg, 198255, Russia

Sapienza University of Rome, Piazzale Aldo Moro 5, 00185 Rome, Italy

School of Medicine, National Center for Asbestos Related Research, University of Western Australia, Nedlands, WA, Australia 6009

Sir Peter MacCallum Department of Oncology, University of Melbourne, Parkville, 3050, Victoria, Australia

St. Petersburg Academic University RAS, 8/3 Khlopin Str., St. Petersburg, 194021, Russia

Stanford University, Palo Alto, CA, USA

Stephenson Cancer Center, University of Oklahoma, Oklahoma City, OK USA

Tayside Tissue Bank, University of Dundee, Scotland UK DD1 9SY

The International Genomics Consortium, 445 N. 5th Street, Phoenix, Arizona 85004

The Ohio State University, Columbus, OH 43210

The Ohio State University Comprehensive Cancer Center, 320 W 10th Avenue, Columbus, OH 43210

The Ohio State University Wexner Medical Center (2012 Kenny Rd, Columbus, OH 43221)

The Oregon Clinic 1111 NE 99th Ave, Portland, OR 97220

The Prince Charles Hospital, UQ Thoracic Research Centre, Australia 4032

The Research Institute at Nationwide Children's Hospital 700 Children's Drive Columbus Ohio 43205

Tufts Medical center, 800 Washington St. Boston MA 02111

UABMC 401 Beacon Pkwy W Birmingham AL 35209

UC Cancer Institute, 200 Albert Sabin Way, Suite 1012, Cincinnati, OH 45267-0502

UCSF-Helen Diller Family Comprehensive Cancer Center, 550 16th St., Mission Hall WS 6532 Box 3211, San Francisco, CA 94143

University Hospital of Giessen and Marburg, Badingerstrasse 3, 35044, Marburg, Germany

University Hospital in Wurzburg, Germany, Oberdurrbacher Strasse 6, 97080, Wurzburg, Germany

University Health Network, 200 Elizabeth Street, Toronto ON M5G 2C4 Canada

University Hospital Essen, University Duisburg-Essen, German Cancer Consortium, Hufelandstr. 55; 45239 Essen, Germany

University Medical Center Hamburg-Eppendorf, Martinistr. 52, D-20246 Hamburg, Germany

University of Abuja Teaching Hospital, Gwagalada, FCT, Nigeria

University of Arizona Tucson Arizona

University of Calgary, Departments of Surgery and Oncology, 1331 - 29th St NW, Calgary, AB, T2N 4N2

University of California San Francisco, 2340 Sutter St Rm S 229, San Francisco CA 94143

University of California, Irvine 333 City Boulevard West Suite 1400 Orange CA 92868

University of Chicago Medicine 5841 S. Maryland Ave. Room G-216, MC 5094|Chicago, IL 60637

University of Cincinnati Cancer Institute, Brain Tumor Clinical Trials, 200 Albert Sabin Way Suite 1012, Cincinnati, OH 45267

University of Cincinnati Cancer Institute, Holmes Bldg., 200 Albert Sabin Way, Ste 1002, Cincinnati, OH 45267-0502

University of Colorado Cancer Center, Aurora, CO, 80111, USA

University of Dundee, Scotland UK DD1 9SY

University of Florence, Viale Pieraccini 6, 50139 Firenze, Italy

University of Hawaii Cancer Center

University of Iowa Hospital & Clinics, 200 Hawkins Drive, Clinical Trials-Data Management, 11510 PFP, Iowa City, IA 52242

University of Iowa Hospital & Clinics, 200 Hawkins Drive, Hematology/Oncology, C32 GH, Iowa City, IA 52242

University of Iowa Hospital & Clinics, 200 Hawkins Drive, ICTS-Informatics, 272 MRF, Iowa City, IA 52242

University of Iowa Hospital & Clinics, 200 Hawkins Drive, Medicine Administration, 380 MRC, Iowa City, IA 52242

University of Iowa Hospital & Clinics, 200 Hawkins Drive, Molecular Pathology, B606 GH, Iowa City, IA 52242

University of Iowa Hospital & Clinics, 200 Hawkins Drive, Pathology, SW247 GH, Iowa City, IA 52242

University of Kansas Cancer Center, 3901 Rainbow Blvd, Kansas City, KS. 66160

University of Kansas Medical Center Kansas City KS 66160

University of Michigan 500 S State St, Ann Arbor, MI 48109

University of Montreal 2900 Edouard Mont petit Blvd, Montreal, QC H3T 1J4, Canada

University of New Mexico Albuquerque, New Mexico 87131

University of Pennsylvania Philadelphia, PA 19104

University of Pittsburgh, Department of Cardiothoracic Surgery,200 Lothrop St, Suite C-800, Pittsburgh, Pennsylvania 15213

University of Pittsburgh, Department of Pathology, Pittsburgh, Pennsylvania 15213

University of Sheffield Western Bank, Sheffield S10 2TN, UK

University of Washington Seattle, WA 98105

UPR Comprehensive Cancer Center Biobank; University of Puerto Rico Comprehensive Cancer Center, Celso Barbosa St. Medical Center Area, San Juan, PR 00936

Urologic Oncology Branch, Center for Cancer Research, National Cancer Institute, Building 10, Room 1-5940, Bethesda, MD 20892-1107

Valley Health System, 1 Valley Health Plaza, Paramus, NJ 07652

Vanderbilt University Medical Center 1211 Medical Center Dr, Nashville, TN 37232

Washington University School of Medicine, 600 S. Taylor Ave, St. Louis, MO 63110

Weill Cornell Medical College, New York, NY 10065

References

Adalsteinsson VA, Ha G, Freeman SS, Choudhury AD, Stover DG, Parsons HA, Gydush G, Reed SC, Rotem D, Rhoades J, et al. Scalable whole-exome sequencing of cell-free DNA reveals high concordance with metastatic tumors. Nat Commun. 2017; 8:1324. [PubMed: 29109393]

Aran D, Hu Z, Butte AJ. xCell: digitally portraying the tissue cellular heterogeneity landscape. Genome Biol. 2017; 18:220. [PubMed: 29141660]

Barkauskas CE, Chung MI, Fioret B, Gao X, Katsura H, Hogan BL. Lung organoids: current uses and future promise. Development. 2017; 144:986–997. [PubMed: 28292845]

Bass AJ, Watanabe H, Mermel CH, Yu S, Perner S, Verhaak RG, Kim SY, Wardwell L, Tamayo P, Gat-Viks I, et al. SOX2 is an amplified lineage-survival oncogene in lung and esophageal squamous cell carcinomas. Nat Genet. 2009; 41:1238–1242. [PubMed: 19801978]

Beroukhim R, Getz G, Nghiemphu L, Barretina J, Hsueh T, Linhart D, Vivanco I, Lee JC, Huang JH, Alexander S, et al. Assessing the significance of chromosomal aberrations in cancer: methodology and application to glioma. Proc Natl Acad Sci USA. 2007; 104:20007–20012. [PubMed: 18077431]

Beroukhim R, Mermel CH, Porter D, Wei G, Raychaudhuri S, Donovan J, Barretina J, Boehm JS, Dobson J, Urashima M, et al. The landscape of somatic copy-number alteration across human cancers. Nature. 2010; 463:899–905. [PubMed: 20164920]

Bonney ME, Moriya H, Amon A. Aneuploid proliferation defects in yeast are not driven by copy number changes of a few dosage-sensitive genes. Gene Dev. 2015; 29:898–903. [PubMed: 25934502]

Brennan CW, Verhaak RG, McKenna A, Campos B, Noushmehr H, Salama SR, Zheng S, Chakravarty D, Sanborn JZ, Berman SH, et al. The somatic genomic landscape of glioblastoma. Cell. 2013; 155:462–477. [PubMed: 24120142]

Buccitelli C, Salgueiro L, Rowald K, Sotillo R, Mardin BR, Korbel JO. Pan-cancer analysis distinguishes transcriptional changes of aneuploidy from proliferation. Genome Res. 2017; 27:501–511. [PubMed: 28320919]

Cai Y, Crowther J, Pastor T, Abbasi Asbagh L, Baietti MF, De Troyer M, Vazquez I, Talebi A, Renzi F, Dehairs J, et al. Loss of chromosome 8p governs tumor progression and drug response by altering lipid metabolism. Cancer Cell. 2016; 29:751–766. [PubMed: 27165746]

Cairncross G, Wang M, Shaw E, Jenkins R, Brachman D, Buckner J, Fink K, Souhami L, Laperriere N, Curran W, et al. Phase III trial of chemoradiotherapy for anaplastic oligodendroglioma: long-term results of RTOG 9402. J Clin Oncol. 2013; 31:337–343. [PubMed: 23071247]

Campbell JD, Alexandrov A, Kim J, Wala J, Berger AH, Pedamallu CS, Shukla SA, Guo G, Brooks AN, Murray BA, et al. Distinct patterns of somatic genome alterations in lung adenocarcinomas and squamous cell carcinomas. Nat Genet. 2016; 48:607–616. [PubMed: 27158780]

Carter SL, Cibulskis K, Helman E, McKenna A, Shen H, Zack T, Laird PW, Onofrio RC, Winckler W, Weir BA, et al. Absolute quantification of somatic DNA alterations in human cancer. Nat Biotechnol. 2012; 30:413–421. [PubMed: 22544022]

Carter SL, Eklund AC, Kohane IS, Harris LN, Szallasi Z. A signature of chromosomal instability inferred from gene expression profiles predicts clinical outcome in multiple human cancers. Nat Genet. 2006; 38:1043–1048. [PubMed: 16921376]

Ciriello G, Miller ML, Aksoy BA, Senbabaoglu Y, Schultz N, Sander C. Emerging landscape of oncogenic signatures across human cancers. Nat Genet. 2013; 45:1127–1133. [PubMed: 24071851]

Davoli T, Uno H, Wooten EC, Elledge SJ. Tumor aneuploidy correlates with markers of immune evasion and with reduced response to immunotherapy. Science. 2017; 355

Dobin A, Davis CA, Schlesinger F, Drenkow J, Zaleski C, Jha S, Batut P, Chaisson M, Gingeras TR. STAR: ultrafast universal RNA-seq aligner. Bioinformatics. 2013; 29:15–21. [PubMed: 23104886]

Hagerstrand D, Tong A, Schumacher SE, Ilic N, Shen RR, Cheung HW, Vazquez F, Shrestha Y, Kim SY, Giacomelli AO, et al. Systematic interrogation of 3q26 identifies TLOC1 and SKIL as cancer drivers. Cancer Discov. 2013; 3:1044–1057. [PubMed: 23764425]

Hoadley KA, Yau C, Wolf DM, Cherniack AD, Tamborero D, Ng S, Leiserson MDM, Niu B, McLellan MD, Uzunangelov V, et al. Multiplatform analysis of 12 cancer types reveals molecular classification within and across tissues of origin. Cell. 2014; 158:929–944. [PubMed: 25109877]

Holland AJ, Cleveland DW. Boveri revisited: chromosomal instability, aneuploidy and tumorigenesis. Nat Rev Mol Cell Biol. 2009; 10:478–487. [PubMed: 19546858]

Hsu PD, Scott DA, Weinstein JA, Ran FA, Konermann S, Agarwala V, Li Y, Fine EJ, Wu X, Shalem O, et al. DNA targeting specificity of RNA-guided Cas9 nucleases. Nature Biotechnol. 2013; 31:827–832. [PubMed: 23873081]

Hung J, Kishimoto Y, Sugio K, Virmani A, McIntire DD, Minna JD, Gazdar AF. Allele-specific chromosome 3p deletions occur at an early stage in the pathogenesis of lung carcinoma. JAMA. 1995; 273:558–563. [PubMed: 7837389]

Lai D, Ha G, Shah S. HMMcopy: Copy number prediction with correction for GC and mappability bias for HTS data. R package version 1.18.0. 2016

Larsson LG. Oncogene- and tumor suppressor gene-mediated suppression of cellular senescence. Semin Cancer Biol. 2011; 21:367–376. [PubMed: 22037160]

Li B, Dewey CN. RSEM: accurate transcript quantification from RNA-Seq data with or without a reference genome. BMC Bioinformatics. 2011; 12:323. [PubMed: 21816040]

Liu Y, Chen C, Xu Z, Scuoppo C, Rillahan CD, Gao J, Spitzer B, Bosbach B, Kastenhuber ER, Baslan T, et al. Deletions linked to TP53 loss drive cancer through p53-independent mechanisms. Nature. 2016; 531:471–475. [PubMed: 26982726]

Lundberg AS, Randell SH, Stewart SA, Elenbaas B, Hartwell KA, Brooks MW, Fleming MD, Olsen JC, Miller SW, Weinberg RA, et al. Immortalization and transformation of primary human airway epithelial cells by gene transfer. Oncogene. 2002; 21:4577–4586. [PubMed: 12085236]

Mali P, Esvelt KM, Church GM. Cas9 as a versatile tool for engineering biology. Nat Methods. 2013; 10:957–963. [PubMed: 24076990]

Mitelman F. Recurrent chromosome aberrations in cancer. Mutat Res. 2000; 462:247–253. [PubMed: 10767636]

Pedregosa F, Varoquaux G, Gramfort A, Michel V, Thirion B, Grisel O, Blondel M, Prettenhofer P, Weiss R, Dubourg V, et al. Scikit-learn: Machine learning in Python. J Mach Learn Res. 2011; 12:2825–2830.

Ried T, Hu Y, Difilippantonio MJ, Ghadimi BM, Grade M, Camps J. The consequences of chromosomal aneuploidy on the transcriptome of cancer cells. Biochim Biophys Acta. 2012; 1819:784–793. [PubMed: 22426433]

Rizvi NA, Hellmann MD, Snyder A, Kvistborg P, Makarov V, Havel JJ, Lee W, Yuan J, Wong P, Ho TS, et al. Mutational landscape determines sensitivity to PD-1 blockade in non-small cell lung cancer. Science. 2015; 348:124–128. [PubMed: 25765070]

Robinson MD, McCarthy DJ, Smyth GK. edgeR: a Bioconductor package for differential expression analysis of digital gene expression data. Bioinformatics. 2010; 26:139–140. [PubMed: 19910308]

Santaguida S, Richardson A, Iyer DR, M'Saad O, Zasadil L, Knouse KA, Wong YL, Rhind N, Desai A, Amon A. Chromosome mis-segregation generates cell-cycle-arrested cells with complex

karyotypes that are eliminated by the immune system. Dev Cell. 2017; 41:638–651. e5. [PubMed: 28633018]

Senovilla L, Vitale I, Martins I, Tailler M, Pailleret C, Michaud M, Galluzzi L, Adjemian S, Kepp O, Niso-Santano M, et al. An immunosurveillance mechanism controls cancer cell ploidy. Science. 2012; 337:1678–1684. [PubMed: 23019653]

Sheltzer JM, Blank HM, Pfau SJ, Tange Y, George BM, Humpton TJ, Brito IL, Hiraoka Y, Niwa O, Amon A. Aneuploidy drives genomic instability in yeast. Science. 2011; 333:1026–1030. [PubMed: 21852501]

Sheltzer JM, Ko JH, Replogle JM, Habibe Burgos NC, Chung ES, Meehl CM, Sayles NM, Passerini V, Storchova Z, Amon A. Single-chromosome gains commonly function as tumor suppressors. Cancer Cell. 2017; 31:240–255. [PubMed: 28089890]

Sheltzer JM, Torres EM, Dunham MJ, Amon A. Transcriptional consequences of aneuploidy. Proc Natl Acad Sci USA. 2012; 109:12644–12649. [PubMed: 22802626]

Stingele S, Stoehr G, Peplowska K, Cox J, Mann M, Storchova Z. Global analysis of genome, transcriptome and proteome reveals the response to aneuploidy in human cells. Mol Syst Biol. 2012; 8:608. [PubMed: 22968442]

Subramanian A, Tamayo P, Mootha VK, Mukherjee S, Ebert BL, Gillette MA, Paulovich A, Pomeroy SL, Golub TR, Lander ES, et al. Gene set enrichment analysis: A knowledge-based approach for interpreting genome-wide expression profiles. Proc Natl Acad Sci USA. 2005; 102:15545–15550. [PubMed: 16199517]

Sundaresan V, Ganly P, Hasleton P, Rudd R, Sinha G, Bleehen NM, Rabbitts P. p53 and chromosome 3 abnormalities, characteristic of malignant lung tumours, are detectable in preinvasive lesions of the bronchus. Oncogene. 1992; 7:1989–1997. [PubMed: 1408139]

Tang YC, Amon A. Gene copy-number alterations: A cost-benefit analysis. Cell. 2013; 152:394–405. [PubMed: 23374337]

Taylor-Weiner A, Zack T, O'Donnell E, Guerriero JL, Bernard B, Reddy A, Han GC, AlDubayan S, Amin-Mansour A, Schumacher SE, et al. Genomic evolution and chemoresistance in germ-cell tumours. Nature. 2016; 540:114–118. [PubMed: 27905446]

Kandoth C, Schultz N, Cherniack AD, Akbani R, Liu Y, Shen H, Robertson AG, Pashtan I, Shen R, et al. The Cancer Genome Atlas (TCGA) Research Network. Integrated genomic characterization of endometrial carcinoma. Nature. 2013; 497:67–73. [PubMed: 23636398]

Brat DJ, Verhaak RG, Aldape KD, Yung WK, Salama SR, Cooper LA, Rheinbay E, Miller CR, Vitucci M, et al. The Cancer Genome Atlas (TCGA) Research Network. Comprehensive, Integrative Genomic Analysis of Diffuse Lower-Grade Gliomas. New Engl J Med. 2015; 372:2481–2498. [PubMed: 26061751]

Topalian SL, Taube JM, Anders RA, Pardoll DM. Mechanism-driven biomarkers to guide immune checkpoint blockade in cancer therapy. Nat Rev Cancer. 2016; 16:275–287. [PubMed: 27079802]

Torres EM, Sokolsky T, Tucker CM, Chan LY, Boselli M, Dunham MJ, Amon A. Effects of aneuploidy on cellular physiology and cell division in haploid yeast. Science. 2007; 317:916–924. [PubMed: 17702937]

Uno N, Hiramatsu K, Uno K, Komoto S, Kazuki Y, Oshimura M. CRISPR/Cas9-induced transgene insertion and telomere-associated truncation of a single human chromosome for chromosome engineering in CHO and A9 cells. Sci Rep. 2017; 7:12739. [PubMed: 28986519]

Weaver BA, Cleveland DW. Does aneuploidy cause cancer? Curr Opin Cell Biol. 2006; 18:658–667. [PubMed: 17046232]

Williams BR, Prabhu VR, Hunter KE, Glazier CM, Whittaker CA, Housman DE, Amon A. Aneuploidy affects proliferation and spontaneous immortalization in mammalian cells. Science. 2008; 322:703–709. [PubMed: 18974345]

Wistuba II, Behrens C, Virmani AK, Mele G, Milchgrub S, Girard L, Fondon JW 3rd, Garner HR, McKay B, Latif F, et al. High resolution chromosome 3p allelotyping of human lung cancer and preneoplastic/preinvasive bronchial epithelium reveals multiple, discontinuous sites of 3p allele loss and three regions of frequent breakpoints. Cancer Res. 2000; 60:1949–1960. [PubMed: 10766185]

Xue W, Kitzing T, Roessler S, Zuber J, Krasnitz A, Schultz N, Revill K, Weissmueller S, Rappaport AR, Simon J, et al. A cluster of cooperating tumor-suppressor gene candidates in chromosomal deletions. Proc Natl Acad Sci USA. 2012; 109:8212–8217. [PubMed: 22566646]

Zabarovsky ER, Lerman MI, Minna JD. Tumor suppressor genes on chromosome 3p involved in the pathogenesis of lung and other cancers. Oncogene. 2002; 21:6915–6935. [PubMed: 12362274]

Zack TI, Schumacher SE, Carter SL, Cherniack AD, Saksena G, Tabak B, Lawrence MS, Zhang CZ, Wala J, Mermel CH, et al. Pan-cancer patterns of somatic copy number alteration. Nat Genet. 2013; 45:1134–1140. [PubMed: 24071852]

Highlights

- Aneuploidy, whole chromosome or chromosome-arm imbalance, occurs in 88% of cancers
- Aneuploidy correlates with cell cycle genes and anti-correlates with immune levels
- Patterns of aneuploidy alterations are tumor-type specific
- Engineered chromosome 3p deletion does not promote proliferation in human lung cells

Significance

Although its universality makes aneuploidy a salient feature of cancer genomes, the functional significance of cancer aneuploidy remains a mystery. Powerful technologies for genome analysis and genome engineering now make the study of aneuploidy more tractable. Here, we look across cancer to identify universal and cancer-type specific characteristics of aneuploidy which further hint at its importance for the process of cancer pathogenesis. Furthermore, the ability to engineer aneuploid chromosome arms will now enable the development of more complex cellular models to generate and investigate the proliferative and survival impact of cancer aneuploidy.

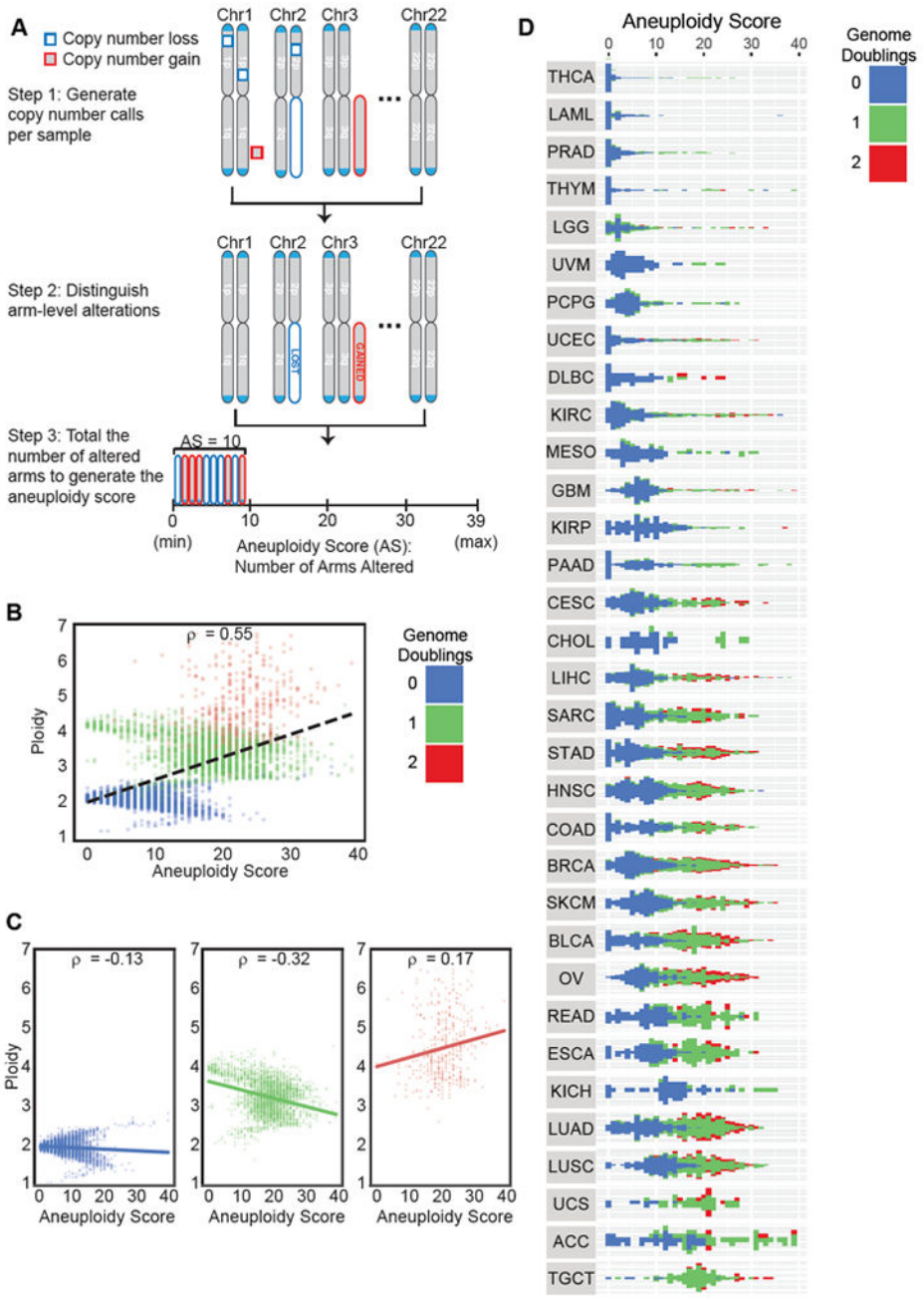

Figure 1. Aneuploidy correlates with ploidy, genome doubling status, and tumor type

(A) Schematic of aneuploidy score. Step 1 is to generate copy number calls per sample, including somatic copy number alterations (SCNAs) of all sizes. Step 2 is to distinguish arm-level alterations within these SCNAs. Step 3 is to total the number of altered arms to generate the aneuploidy score.

(B) Each tumor sample is organized by genome doubling status (blue = not doubled, green = 1 genome doubling, red = 2 or more genome doublings). X-axis is aneuploidy score, the sum of the number of altered chromosome arms. Y-axis is ploidy as determined by ABSOLUTE. Spearman's rank correlation coefficient = 0.55.

(C) X-axis is aneuploidy score, the sum of the number of altered chromosome arms. Y-axis is ploidy as determined by ABSOLUTE. Samples are separated by whole genome doubling status: samples without genome doubling (left, blue, Spearman's rank correlation coefficient = -0.13), samples with one genome doubling (middle, green, Spearman's rank correlation coefficient = -0.32), and samples with 2 or more genome doublings (right, red, Spearman's rank correlation coefficient = 0.17).

(D) Each tumor sample is organized by tumor type and genome doubling status (blue = not doubled, green = 1 genome doubling, red = 2 or more genome doublings). Samples are organized by tumor type, and ranked from least to most aneuploid samples within a tumor type. X-axis is aneuploidy score, y-axis is sample number.

See also Figure S1 and Tables S1 and S2.

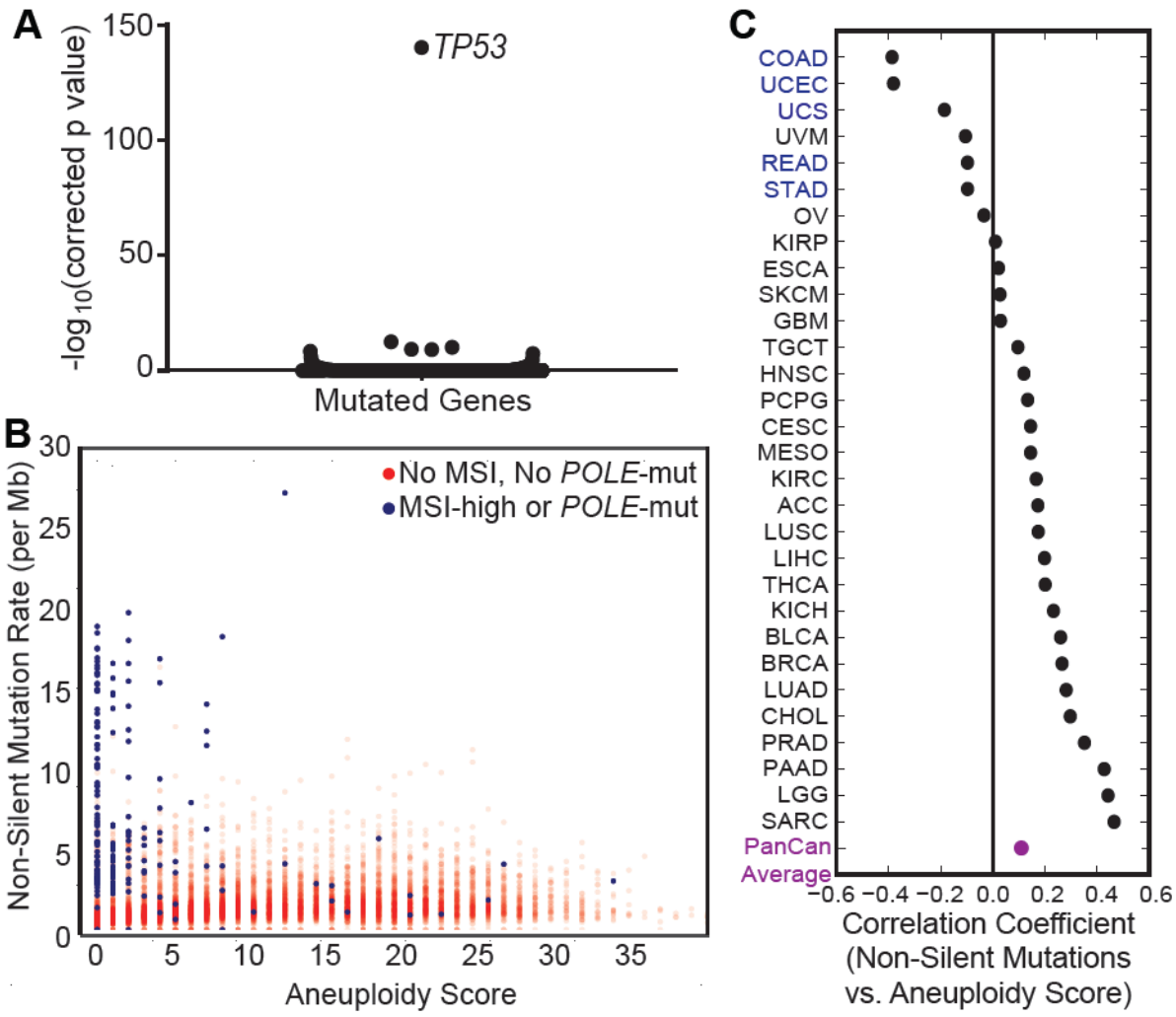

Figure 2. Aneuploidy score correlates with *TP53* mutations and overall mutation rate

(A) Y-axis is -$\log_{10}$ Bonferroni corrected p value for linear model coefficient of aneuploidy score. Dots represent every mutated gene.

(B) X-axis is aneuploidy score. Y-axis is rate of non-silent mutations per megabase (square root). Blue samples have been called as microsatellite instability (MSI)-high or *POLE* mutated, whereas red samples do not have these features or have not been called.

(C) Spearman correlation coefficients for aneuploidy score and mutation rate across TCGA tumor types, arranged from smallest to largest value. Tumor types in blue have MSI-high or *POLE* mutated samples. Average of correlation coefficients across cancer types is in purple. See also Figure S2 and Tables S3 and S4.

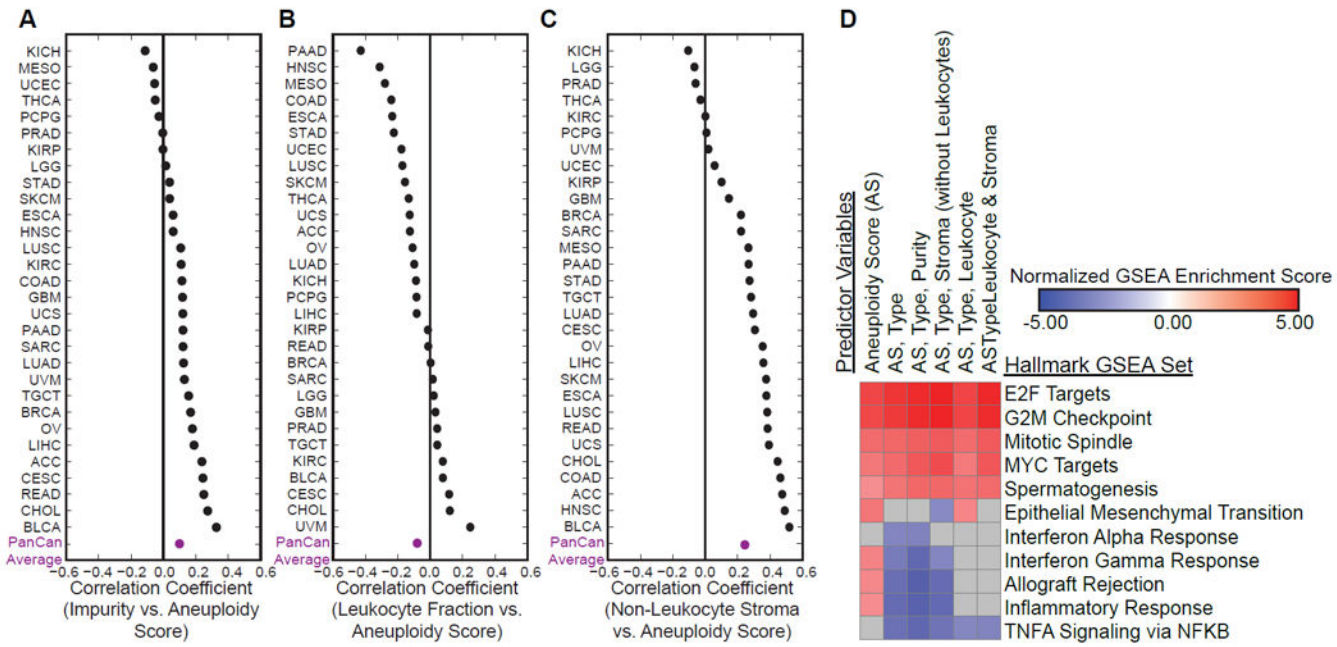

Figure 3. Aneuploidy score negatively correlates with immune infiltrate, which contributes to decreased expression of immune genes

(A) Spearman correlation coefficients for aneuploidy score and impurity across TCGA tumor types, arranged from smallest to largest value. Average of correlation coefficients across tumor types is in purple.

(B) Spearman correlation coefficients for aneuploidy score and leukocyte fraction across TCGA tumor types, arranged from smallest to largest value. Average of correlation coefficients across tumor types is in purple.

(C) Spearman correlation coefficients for aneuploidy score and non-leukocyte stroma across TCGA tumor types, arranged from smallest to largest value. Average of correlation coefficients across tumor types is in purple.

(D) Heatmap of normalized enrichment scores for Hallmark gene sets in GSEA (Gene Set Enrichment Analysis), with FWER (family-wise error rate) p value < 0.01. Gray = not significant or not enriched. Predictor variables describe variables included in linear regression model for gene expression. Pathways are those identified from genes with significant coefficients in linear regression analysis.

See also Figure S2 and Tables S4, S5, and S6.

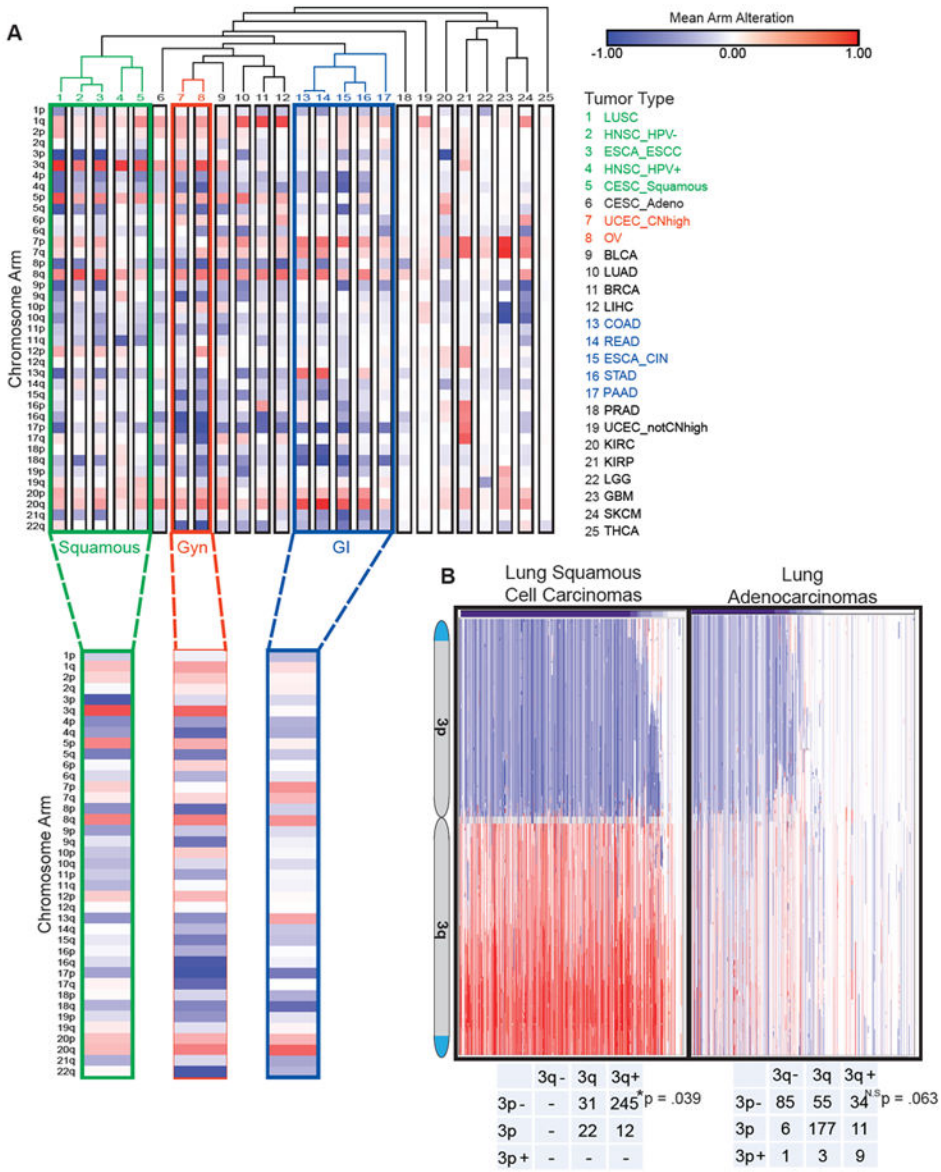

Figure 4. Patterns of arm-level alterations cluster by tumor site, tissue of origin, and squamous morphology

(A) Matrix of mean arm-level alteration within each tumor type/subtype. Hierarchical clustering of tumor type by Pearson's method.

(B) Integrated genomics viewer (IGV) plots of chromosome 3 copy number alterations in lung squamous cell carcinoma or lung adenocarcinoma. Blue = loss, red = gain. Numbers for lung squamous and lung adenocarcinoma samples that had arm calls for both 3p and 3q. P values represent chi-square test for enrichment of co-occurrence of chromosome 3p loss and chromosome 3q gain.

See also Figure S3 and Tables S7 and S8.

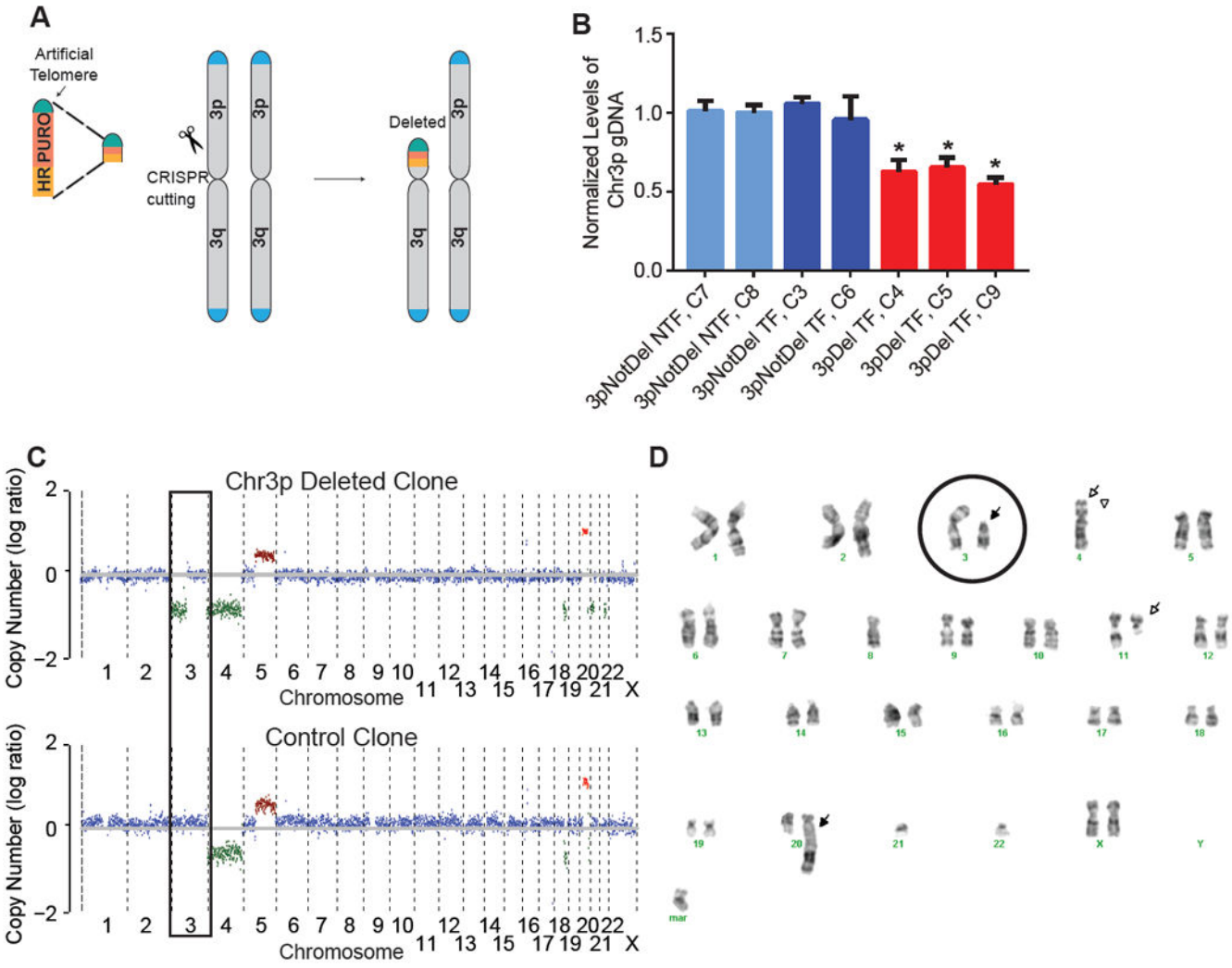

Figure 5. CRISPR-based approach can delete a chromosome arm in human immortalized cells

(A) Schematic of CRISPR and recombination based approach to delete chr_3p *in vitro*. A linearized plasmid containing homologous DNA, a puromycin selection marker, and an artificial telomere is co-transfected with a CRISPR-Cas9 construct to target DNA sequence adjacent to the centromere. Upon transfection, a double-strand break is produced and repaired by homologous directed recombination, removing a chromosome arm and replacing it with an artificial telomere.

(B) qPCR measuring chr_3p gDNA normalized to chr_3q gDNA in single cell clones. Bars represent means with error bars +/- standard deviation. Light blue = single cell clones that were not transfected (NTF) and did not have chr_3p deletion, dark blue = single cell clones that were transfected (TF) but did not have chr_3p deletion, and red = single cell clones that were transfected and have chr_3p deletion. (* = p value < 0.05)

(C) Whole genome sequencing output of HMMCopy, for one chr_3p deleted cell clone (top) and a non-deleted control clone (bottom).

(D) Karyotype of one chr_3p deleted cell clone. Chromosome 3 is circled, and arrows point to chromosomal abnormalities. Mar = marker chromosome.

See also Figure S4.

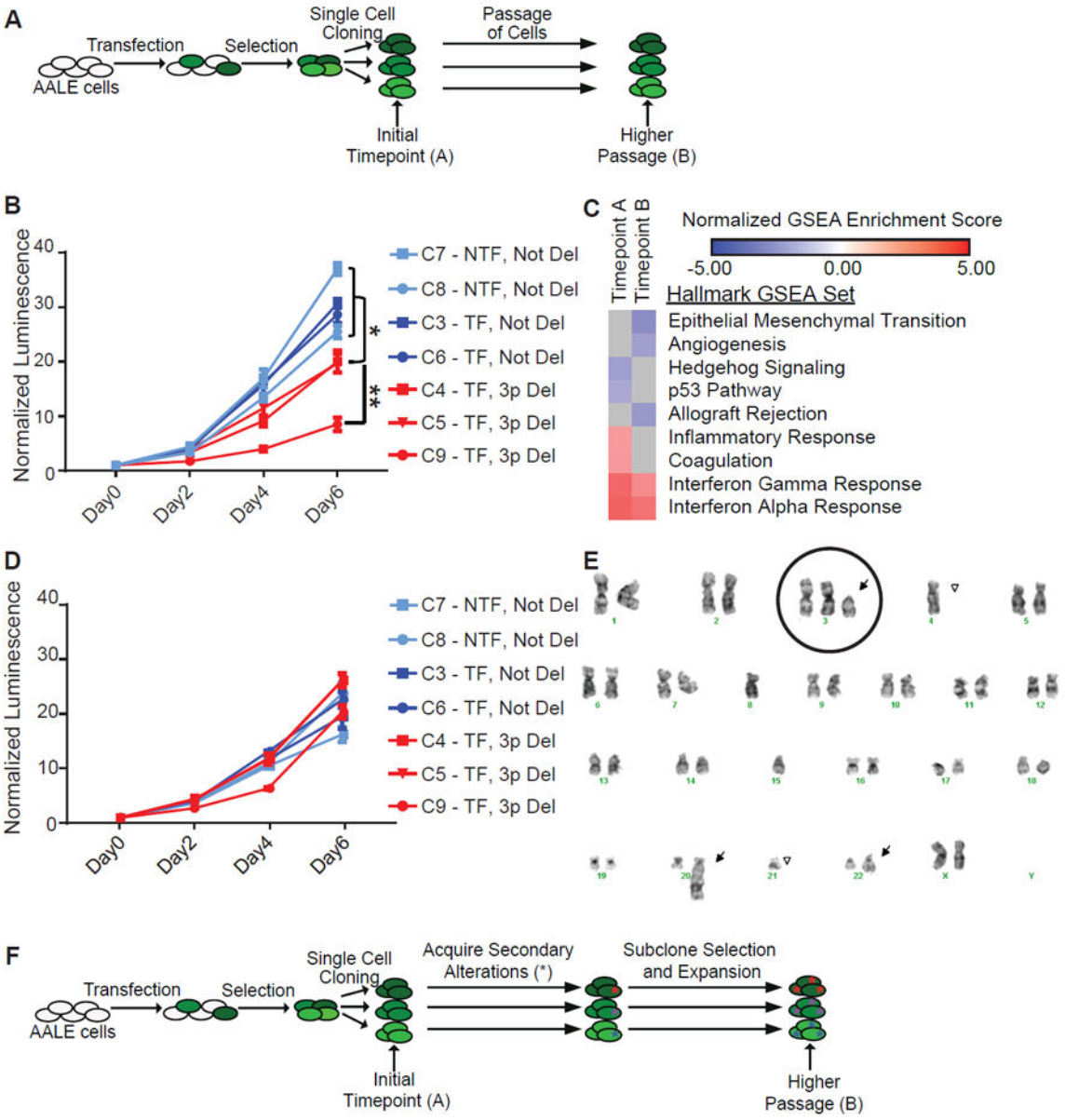

Figure 6. Chromosome 3p lung cells initially have slower proliferation, but normalize over time

(A) AALE cells were transfected, and one day later cells were selected with puromycin for cells that had incorporated transfected DNA. Cells were single cell cloned to isolate chr_3p deleted clones, and assayed before and after extensive passaging.

(B) Proliferation curves were generated using CellTiter-Glo over 6 days (x-axis). Y-axis is relative luminescence units, normalized to Day 0. Data plotted are means with error bars +/- standard deviation. (* = p value < 0.01, ** = p value < 0.001) Cells were from Timepoint A.

(C) Heatmap of normalized enrichment scores for Hallmark gene sets in GSEA.

(D) Proliferation curves were generated using CellTiter-Glo over 6 days (x-axis). Y-axis is relative luminescence units, normalized to Day 0. Data plotted are means with error bars +/- standard deviation. Cells were from the higher passage population.

(E) Karyotype from one of the chromosome 3p deleted clones. Chromosome 3 is circled, and arrows point to chromosomal abnormalities.
(F) During passaging, cells have gained additional changes (*) to adapt to chr_3p deletion. See also Figure S4.

Table 1

Summary of results

Aneuploidy and Ploidy
• Across 10,522 pan-cancer samples, the correlation coefficient between ploidy and aneuploidy score is 0.55.
• Across 6,800 samples without genome doubling, the correlation coefficient is -0.13.
• Across 3,242 samples with one genome doubling, the correlation coefficient is -0.32.
• Across 480 samples with two or more genome doublings, the correlation coefficient is 0.17.
Aneuploidy and Mutations
• Across 9,702 samples (with copy number and mutation data) and corrected by tumor type and mutation rate, TP53 mutation is enriched in samples with higher aneuploidy, with a coefficient of 0.126 and a Bonferroni corrected p value of $5.58*10^{-141}$.
• Across 9,766 pan-cancer samples in 30 tumor types (with copy number, mutation rate, and leukocyte fraction data), the correlation coefficient between non-silent mutation rate and aneuploidy score is 0.336.
• Across 191 samples with high microsatellite instability or *POLE* mutations, the correlation coefficient between non-silent mutation rate and aneuploidy score is -0.239
• Across 9,575 samples without high microsatellite instability or *POLE* mutations, the correlation coefficient between non-silent mutation rate and aneuploidy score is 0.379.
• Across 9,766 pan-cancer samples, the average tumor-type correlation coefficient between impurity and aneuploidy score is 0.089.
• Across 9,766 pan-cancer samples, the average tumor-type correlation coefficient between leukocyte fraction and aneuploidy score is -0.077.
• Across 9,766 pan-cancer samples, the average tumor-type correlation coefficient between non-leukocyte stroma and aneuploidy score is 0.241.
Chromosome Arm-Alterations and Cross-Tumor Clusters
• Clustering 25 tumor subtypes revealed a group of gastrointestinal (endoderm) tumors, including colon adenocarcinoma, rectal adenocarcinoma, esophageal adenocarcinoma, stomach adenocarcinoma, and pancreatic adenocarcinoma. The Pearson's correlations range from 0.37 to 0.99.
• Clustering revealed a group of gynecological (mesoderm) tumors, including endometrial carcinoma with high copy number levels and ovarian cancers. The Pearson's correlation coefficient is 0.90.
• Clustering revealed a group of squamous cell carcinomas (ectoderm), including lung squamous cell carcinoma, head and neck squamous cell carcinoma, esophageal squamous carcinoma, and cervical squamous carcinoma. The Pearson's correlation coefficient ranges from 0.58 to 0.94.
Phenotypes of Chromosome 3p Deletion
• Chromosome 3p deletion and chromosome 3q gain are significantly enriched in lung squamous cell carcinoma, with a p value of 0.039.
• Chromosome 3p deletion does not induce apoptosis.
• Chromosome 3p deletion induces slowed cell cycle (more cells in G1), with a p value of 0.0006.
• Chromosome 3p deletion initially induces slower cellular proliferation (p value < 0.0017).
• Chromosome 3 duplication occurs in chromosome 3p deleted cells.

KEY RESOURCES TABLE

REAGENT or RESOURCE	SOURCE	IDENTIFIER
Critical Commercial Assays		
Nextera DNA Sample Preparation Kit	Illumina	Catalog: FC-121-1030
NEBNext Ultra Directional RNA Library Prep Kit	New England Biolabs	Catalog: E7420S
QIAamp DNA Mini Kit	Qiagen	Catalog: 51304
Qiagen RNeasy Mini Kit	Qiagen	Catalog: 74104
CellTiter-Glo Luminescence Viability Assay	VWR	Catalog: PAG7572
Deposited Data		
Raw data files for RNA-sequencing of *in vitro* AALE clones	This paper	https://www.ncbi.nlm.nih.gov/Traces/study/?acc=SRP133935
Raw data files for DNA-sequencing of *in vitro* AALE clones	This paper	https://www.ncbi.nlm.nih.gov/Traces/study/?acc=SRP133935
Experimental Models: Cell Lines		
Immortalized Lung Epithelial Cells (AALE)	Lundberg et al., 2002	#N/A
Oligonucleotides		
Chr_3p CRISPR (5' TGATCAGTCAGGTAAGGATG 3')	This paper	#N/A
Recombination PCR Forward (5'CTACCCGCTTCCATTGCTCA 3')	This paper	#N/A
Recombination PCR Reverse (5'TTGGTTGAGCAGTTGGACAT 3')	This paper	#N/A
Chr_3p qPCR Forward (5' ACAATCCAAACTAGCATGCACA 3')	This paper	#N/A
Chr_3p qPCR Reverse (5' AGCGTTAGAGGGAGGGGAG 3')	This paper	#N/A
Chr_3q qPCR Forward (5' CGTGTCCGGGGTAGATCTTG 3')	This paper	#N/A
Chr_3p qPCR Reverse (5' GCTTACATCCTCGGGCAGAA 3')	This paper	#N/A
Software and Algorithms		
ABSOLUTE	Carter et al., 2012	Version 1.5
Python Package SciKit-Learn	Pedregosa et al., 2011	Version 0.16.1
Python Package scipy stats	www.scipy.org	Version 0.19.0
edgeR	Robinson et al., 2010	
STAR	Dobin et al., 2013	
RSEM	Li and Dewey, 2011	
GSEA	Subramanian et al., 2005	Version 3.0

HMMCopy	Lai et al., 2016	
IchorCNA	Adalsteinsson et al., 2017	
Morpheus	https://software.broadinstitute.org/morpheus/index.html	